Title

An Opaque Cell-Specific Expression Program of Secreted Proteases and Transporters Allows Cell-Type Cooperation in Candida albicans

Journal

Genetics, 216(2)

ISSN

0016-6731

Authors

Lohse, Matthew B

Brenes, Lucas R

Ziv, Naomi

et al.

Publication Date

2020-10-01

DOI

10.1534/genetics.120.303613

Peer reviewed

An Opaque Cell-Specific Expression Program of Secreted Proteases and Transporters Allows Cell-Type Cooperation in *Candida albicans*

Matthew B. Lohse,* Lucas R. Brenes,*,[1] Naomi Ziv,* Michael B. Winter,[†,2] Charles S. Craik,[†] and Alexander D. Johnson*,[3]

*Department of Microbiology and Immunology and [†]Department of Pharmaceutical Chemistry, University of California, San Francisco, California 94143

ABSTRACT An unusual feature of the opportunistic pathogen *Candida albicans* is its ability to switch stochastically between two distinct, heritable cell types called white and opaque. Here, we show that only opaque cells, in response to environmental signals, massively upregulate a specific group of secreted proteases and peptide transporters, allowing exceptionally efficient use of proteins as sources of nitrogen. We identify the specific proteases [members of the secreted aspartyl protease (*SAP*) family] needed for opaque cells to proliferate under these conditions, and we identify four transcriptional regulators of this specialized proteolysis and uptake program. We also show that, in mixed cultures, opaque cells enable white cells to also proliferate efficiently when proteins are the sole nitrogen source. Based on these observations, we suggest that one role of white-opaque switching is to create mixed populations where the different phenotypes derived from a single genome are shared between two distinct cell types.

KEYWORDS white-opaque switching; fungal pathogenesis; microbiome; protease

PROTEASE secretion by pathogens plays an important role in many aspects of host–pathogen interactions, including colonization, tissue damage, and interference with host immune responses (Blom *et al.* 2009; Koziel and Potempa 2013; Pietrocola *et al.* 2017). Secreted proteases also contribute to nutrient acquisition; examples include amino acid acquisition by *Legionella pneumophila* (White *et al.* 2018) and carbon acquisition by *Pseudomonas aeruginosa* (Diggle *et al.* 2007). Secreted proteases are also important for the most prevalent fungal pathogen of humans, *Candida albicans*. The secreted aspartyl protease (*SAP*) family from *C. albicans* comprises 13 homologous proteins and has been linked to, among other things, biofilm formation (Winter *et al.* 2016), interactions with bacteria (Dutton *et al.* 2016), adhesion to host cells (Watts *et al.* 1998; Bektic *et al.* 2001; Albrecht *et al.* 2006), protection from host defense proteins (Borg-von Zepelin *et al.* 1998; Gropp *et al.* 2009; Meiller *et al.* 2009; Rapala-Kozik *et al.* 2010, 2015; Bochenska *et al.* 2015; Kozik *et al.* 2015), and activation of host immune responses (Schaller *et al.* 2005; Hornbach *et al.* 2009; Pietrella *et al.* 2010; Pericolini *et al.* 2015; Gabrielli *et al.* 2016). The *SAP* family, especially *SAP2* (Hube *et al.* 1997), has also been linked to *C. albicans*' unusual ability, compared with other fungal species, to utilize proteins [*e.g.*, casein or bovine serum albumin (BSA)] as a nitrogen source (Staib 1965; Nelson and Young 1986). This occurs through the cleavage of proteins into short peptides that are then imported by the oligopeptide transporter (*OPT*) and peptide transporter (*PTR*) families (Reuss and Morschhäuser 2006; Dunkel *et al.* 2013).

Although *C. albicans* is a common component of the human microbiome—asymptomatically colonizing the skin, gastrointestinal tract, and genitourinary tract of healthy individuals—it can cause superficial mucosal or dermal infections as well as disseminated bloodstream infections if the host immune system is compromised or the native microbiome is disrupted (Kennedy and Volz 1985; Wey *et al.* 1988; Wenzel 1995; Calderone and Fonzi 2001; Kullberg and Oude Lashof 2002; Eggimann *et al.* 2003; Gudlaugsson *et al.* 2003; Pappas *et al.* 2004; Achkar and Fries 2010; Kumamoto 2011; Kim and Sudbery 2011). *C. albicans* grows as several distinct cell types *in vitro* and *in vivo*, including yeast, pseudohyphal, and hyphal

doi: https://doi.org/10.1534/genetics.120.303613
Manuscript received April 20, 2020; accepted for publication August 20, 2020; published Early Online August 24, 2020.
Supplemental material available at figshare: https://doi.org/10.25386/genetics.12818894.
[1]Present address: Biology Graduate Program, Massachusetts Institute of Technology, Cambridge, MA 02139.
[2]Present address: CytomX Therapeutics Inc., South San Francisco, CA 94080.
[3]Corresponding author: Department of Microbiology and Immunology, University of California, San Francisco, 600 16th St., MBGH Room N372E, Box 2200, San Francisco, CA 94143-2200. E-mail: ajohnson@cgl.ucsf.edu

cells. In addition, *C. albicans* (and the closely related species *Candida dubliniensis* and *Candida tropicalis*) can switch between two distinct, heritable cell types named "white" and "opaque" (Slutsky *et al.* 1987; Soll *et al.* 1993; Johnson 2003; Pujol *et al.* 2004; Lohse and Johnson 2009; Soll 2009; Morschhäuser 2010; Porman *et al.* 2011). The white and opaque cell types are heritable for many generations, and switching between them occurs approximately once every 10,000 cell divisions under standard laboratory conditions (Rikkerink *et al.* 1988; Bergen *et al.* 1990). Although genetically identical, these two cell types differ in the appearance of their colonies, in their cell morphologies (Figure 1A), as well as in expression of roughly 15% of the genome (Lan *et al.* 2002; Tuch *et al.* 2010). As a result of these expression differences, the two cell types also differ in their abilities to mate (Miller and Johnson 2002), their responses to environmental conditions (Si *et al.* 2013), their metabolic preferences (Lan *et al.* 2002; Ene *et al.* 2016; Dalal *et al.* 2019), and their interactions with the host immune system (Kvaal *et al.* 1997, 1999; Geiger *et al.* 2004; Lohse and Johnson 2008; Sasse *et al.* 2013; Takagi *et al.* 2019). Transcriptional profiling has revealed that several *SAP*s and peptide transporters are differentially expressed between white and opaque cells (*e.g.*, *OPT1* is enriched in white cells, *SAP1* and *OPT4* are enriched in opaque cells) (Hube *et al.* 1994; White and Agabian 1995; Lan *et al.* 2002; Tuch *et al.* 2010; Hernday *et al.* 2013). It has also been shown that opaque cells proliferate better than white cells when dipeptides, tripeptides, or BSA are the sole nitrogen source (Kvaal *et al.* 1999; Lan *et al.* 2002; Ene *et al.* 2016).

In this work, we show that opaque cells have a specialized program that is induced when protein present in the environment is the sole source of nitrogen. This inducible program, which is not observed in white cells, includes the massive upregulation of several specific SAP proteins along with a series of peptide transporters. We show that this induced response is needed for the ability of opaque cells to use proteins efficiently as a sole nitrogen source, and, using a series of quadruple and quintuple deletion mutants, we identify the individual SAPs needed for opaque cells to proliferate under these conditions. We also show that Stp1, a known regulator of *SAP2* in white cells (Martínez and Ljungdahl 2005), works in combination with the white-opaque regulators Wor3 and Efg1 to produce the specialized opaque proteolysis program. Finally, we show that, in mixed cultures of white and opaque cells, opaque cells, even when in the minority, can enable white cells to proliferate efficiently when proteins are the sole nitrogen source. Based on these results, we suggest that one role of white–opaque switching is to create mixed populations where the population characteristics derived from a single genome are shared between two distinct cell types.

Materials and Methods

Supplemental Materials and Methods, Supplemental Results, as well as legends for all Supplemental Figures, Files, and Tables can be found in File S1.

Media and growth conditions

Unless otherwise noted, strains were grown at 25° on synthetic complete medium (6.7 g/liter Yeast Nitrogen Base without Amino Acids (BD #291940)) supplemented with 2% glucose, amino acids (2 g/liter), and uridine (100 μg/ml) (SCD+aa+Uri); plates contained 2% agar. Specific nitrogen source and nitrogen depletion media was prepared immediately before use from 2X S+Uri (3.4 g/liter Yeast Nitrogen Base without Amino Acids or ammonium sulfate (MP Biomedicals, #4027-032), 200 μg/ml uridine), 40% glucose, 5% ammonium sulfate (A2939; Sigma), and 10% protein [bovine serum albumin (BSA; A1470; Sigma), human serum albumin (HSA; A8763; Sigma), hemoglobin (Sigma H2500), or myoglobin (M1882; Sigma)] stocks. Final glucose, ammonium sulfate, and protein concentrations, when present, were 2%, 0.5%, and 1%, respectively. Common combinations included BSA without ammonium sulfate or amino acids (SD+BSA+Uri), ammonium sulfate without BSA or amino acids (SD+AmS+Uri), or medium lacking BSA, ammonium sulfate, and amino acids (SD+Uri). Specific nitrogen source, nitrogen depletion, and specific carbon source liquid media were filtered on 0.45 μm polyethersulfone (PES) filters (#725-2545; Thermo) prior to use. Dulbecco's PBS (D-PBS) lacking calcium chloride and magnesium chloride was procured from the Cell Culture facility at the University of California, San Francisco or Gibco (#14190-136). A list of media used in this study can be found in File S2.

Plasmid construction

The mCherry reporter plasmids were constructed as follows in the pUC19 backbone. In three separate steps, *C. albicans* optimized mCherry taken from pMBL180 (Lohse and Johnson 2016), the *SAT1* selectable marker from pNIM1 (Park and Morschhäuser 2005), and the *RPS1/RP10* homology region from pADH33 (Lohse *et al.* 2013) were inserted between the *Hin*dIII–*Pst*I, *Pst*I–*Bam*HI, and *Bam*HI–*Eco*RI restriction sites, respectively, to create the plasmid pNZ116. The promoters for *OPT1* (1968 bp), *OPT2* (2056 bp), *SAP2* (4522 bp), and *UGA4* (980 bp) were amplified from *C. albicans* SC5314 genomic DNA and added to *Hin*dIII-digested pNZ116 backbone using In-Fusion cloning (#638911; Takara) to generate plasmids pNZ119 (*OPT1*), pNZ120 (*OPT2*), pNZ121 (*SAP2*), and pNZ118 (*UGA4*). The promoter regions extend from the start or stop of the upstream gene (with the exception of p*OPT2* and p*UGA4*, which start 24 and 6 base pairs downstream of that location, respectively) to the ATG at the start of the respective genes. All plasmid sequences were verified by sequencing. A list of oligonucleotides and plasmids used in this study can be found in File S2.

Strain construction

The SC5314-derived *C. albicans* wild-type white and opaque strains used in the proteomic and Multiplex Substrate Profiling by Mass Spectrometry (MSP-MS) experiments have been reported previously (Hernday *et al.* 2013); in brief,

these are *HIS1* and *LEU2* addbacks to the SN152 **a**/α *his1 leu2 arg4* strain (Noble and Johnson 2005) that were then converted to the switching capable **a**/Δ background by deletion of the α copy of the Mating Type Like (*MTL*) locus using pJD1 (Lin *et al.* 2013). The opaque transcriptional regulator knockout library strains (Lohse *et al.* 2016) derive from the same background. The previously reported white and opaque Tef2-GFP and Tef2-mCherry strains (Takagi *et al.* 2019) are derived from the switching capable AHY135 strain (Hernday *et al.* 2013), where the *HIS1* and *LEU2* markers were added back to RZY47, itself a sorbose selected **a**/**a** copy of the SN87 **a**/α *his1 leu2* strain (Noble and Johnson 2005; Zordan *et al.* 2006). *C. albicans* clinical isolates L26 and P37005 (Lockhart *et al.* 2002), *C. dubliniensis* CD36 (Sullivan *et al.* 1995), *C. tropicalis* MYA3404 (Joly *et al.* 1996), the *C. tropicalis* AM2005/0093 derived white-opaque switching strains (Anderson *et al.* 2016), and *Candida parapsilosis* CBS604/ATCC22019 (Guerin *et al.* 1989) have all been reported previously.

Gene deletion and truncation utilized the *SAT1* marker-based CRISPR protocol targeting *Candida maltosa LEU2* as described by Nguyen *et al.* (2017). We used a derivative of the hemizygous *LEU2* strain SNY250 [a derivative of SNY152 (**a**/α *his1 leu2 arg4*) with the *C. dubliniensis HIS1* and *C. maltosa LEU2* gene deletion cassettes integrated at the *C. albicans LEU2* locus] (Noble and Johnson 2005), which was converted to **a**/Δ by deleting the α copy of the MTL using pJD1 (Lin *et al.* 2013). For gene deletions, the 90 bp-annealed donor DNA (dDNA) contains homology to the regions directly upstream and downstream of the targeted ORF. Each dDNA homology arm consists of 44 bp and the two homology arms are separated by a two base pair GG insert added to create a potential gRNA site. For the *STP1* truncation mutant (Δ2–61), the dDNA homology arms flank the targeted amino acids and no GG insert was added. Gene deletions were confirmed by colony PCR reactions verifying the loss of the targeted ORF(s) and truncation mutations were confirmed by sequencing. After confirming the presence of the desired edit(s), the Cas9 ORF-gRNA-*SAT1* cassette was recycled by plating on Leu/His/Arg dropout plates and selecting for recombination events with an intact *CmLEU2* ORF. We selected against both leucine and histidine in order to avoid potential histidine auxotrophies arising during the recombination process (both *CmLEU2* and *CdHIS1* are present at the *CaLEU2* locus in the SNY250-derived background).

The mCherry reporter strains were constructed using *Age*I-HF (NEB R3552L)-linearized reporter plasmids transformed into the SNY250-derived **a**/Δ wild type strain. Colonies were selected for growth on Yeast Extract Peptone Dextrose (YEPD) plates supplemented with 400 μg/ml nourseothricin (clonNAT, WERNER BioAgents, Jena, Germany). Plasmid integration at the *RPS1* (*RP10*) locus was verified by colony PCR across the 5′ and 3′ flanks of the integrated plasmid.

A list of oligonucleotides and strains used in this study can be found in File S2.

Conditioned media processing for MSP-MS and proteomic analyses

Following recovery from glycerol stocks, white and opaque *C. albicans* strains were grown for 7 days on SCD+aa+Uri plates at 25°. Overnight cultures (5 ml, SCD+aa+Uri, 25°) were started from single colonies with no visible switching events. The following morning, cell type homogeneity of the overnight culture was verified by microscopy prior to dilution to OD_{600} = 0.05 in 50 ml of SCD+aa+Uri medium in a 250 ml flask; two independent 50 ml cultures were grown for each strain. Cultures were incubated with shaking at 220 rpm for 24 hr at 25° before harvesting as previously described for planktonic *C. albicans* cultures (Winter *et al.* 2016). In short, cultures were transferred to 50 ml tubes and centrifuged for 10 min at 3500 rpm at 4°. The supernatant was collected, filtered on a 0.45 μm PES filter (#725-2545; Thermo), and flash frozen in liquid nitrogen. A small aliquot was taken from each culture immediately prior to harvesting, diluted, and plated on three SCD+aa+Uri plates, which were incubated for 7 days at 25° and then scored for colony morphology to confirm each culture's cell type.

To prepare samples for analysis, each frozen conditioned medium was thawed on ice, the conditioned media from the two independent cultures of each strain were pooled, and the combined sample was concentrated (using a refrigerated centrifuge) to ∼1 ml on 10 kDa MWCO Amicon Ultra spin filter units (Millipore UFC901024). The concentrated solutions were then diluted to 15 ml with ice cold D-PBS to exchange the buffer and subsequently concentrated to ∼750 μl. These concentrated solutions were then aliquoted, flash frozen in liquid nitrogen, and stored at −80°. Protein concentrations of each solution were quantified using the Bradford assay.

MSP-MS analysis

Substrate specificity profiles were determined for 24 hr conditioned media samples, prepared as described above, from white and opaque cultures from an SC5314-derived *C. albicans* strain using the previously reported MSP-MS assay (O'Donoghue *et al.* 2012; Winter *et al.* 2016, 2017). In short, 20 μg/ml processed conditioned medium and matched no-enzyme controls were assayed at room temperature (∼22°) against a diverse library of 228 tetradecapeptides pooled at 500 nM in D-PBS (pH 7.4) and MES (pH 5.5; 9.5 mM MES, 2.7 mM KCl, 140 mM NaCl). A 30 μl aliquot of each 150 μl assay mixture was removed after 15, 60, and 240 min, quenched with 30 μl of 8 M guanidinium-HCl, and flash frozen in liquid nitrogen. Samples were thawed, acidified to pH 2 by the addition of 1.5 μl of 20% formic acid, desalted with C_{18} Desalting Tips (17014047; Rainin), eluted in 40 μl of a 50:50 acetonitrile (34851; Sigma): water (Fisher W5) mixture with 0.2% formic acid, and then lyophilized. Samples were resuspended in 30 μl of 0.2% formic acid solution prior to mass spectrometry.

Cleavage site identification was performed on an LTQ Orbitrap XL mass spectrometer (Thermo) equipped with a

nanoACQUITY (Waters) ultraperformance LC (UPLC) system and an EASY Spray ion source (Thermo). Reversed-phase chromatography was carried out with an EASY-Spray PepMap C_{18} column (Thermo, ES800; 3 μm bead size, 75 μm × 150 mm). Loading was performed at a 600 nl/min flow rate for 12 min, and then peptide separation was performed at a 300 nl/min flow rate over 63 min with a linear gradient of 2–30% (vol/vol) acetonitrile in 0.1% formic acid followed by a 2 min linear gradient from 30 to 50% acetonitrile. Peptide fragmentation was performed by collision-induced dissociation (CID) on the six most intense precursor ions, with a minimum of 1000 counts, with an isolation width of 2.0 *m/z* and a minimum normalized collision energy of 25. For MS/MS analysis, survey scans were recorded over a range of 325 to 1500 *m/z*. Internal recalibration to polydimethylcyclosiloxane ion (*m/z* = 445.120025) was used for both MS and MS/MS scans. MS peak lists were generated with MSConvert. Data were searched against the 228-member peptide library using the Protein Prospector software (http://prospector.ucsf.edu/prospector/mshome.htm, UCSF) (Chalkley *et al.* 2008) with specified tolerances of 20 ppm for parent ions and 0.8 Da for fragment ions. All cleavages were allowed in the search by designating "no enzyme" specificity. The following variable modifications were used: amino acid (proline, tryptophan, and tyrosine) oxidation and N-terminal pyroglutamate conversion from glutamine. Protein Prospector score thresholds were selected with a minimum protein score of 15 and a minimum peptide score of 15. Maximum expectation values of 0.01 and 0.05 were selected for protein and peptide matches, respectively. Peptides corresponding to cleavage products in the 228-member library (O'Donoghue *et al.* 2015) were selected with inhouse software and imported into iceLogo software v.1.2 (Colaert *et al.* 2009) to generate substrate specificity profiles and Z score calculations as described previously (O'Donoghue *et al.* 2012). Octapeptides corresponding to P4–P4′ were used as the positive data set, and octapeptides corresponding to all possible cleavages in the library (n = 2964) were used as the negative data set. Octapeptide cleavage products identified by the MSP-MS assays with the 228-member library are provided in File S3 in the supplemental material.

Proteomic analysis

Proteomic analysis of conditioned media from planktonic cultures of white and opaque cells from three *C. albicans* backgrounds (SC5314, L26, P37005) was based on previously reported methods (Winter *et al.* 2016). In brief, three samples from 24 hr conditioned media preparations of each strain (3 μg diluted to 40 μl with D-PBS) were prepared as described above and matched on a total protein basis. Conditioned media preparations were incubated for 20 min with 6 M urea (U5378; Sigma) and 10 mM DTT (D0632; Sigma) at 55°, alkylated for 1 hr with 12.5 mM iodoacetamide (I6125; Sigma) at room temperature (~22°), quenched with an additional 10 mM DTT, and diluted 2.5-fold with 25 mM ammonium bicarbonate (100 μl; A6161; Sigma). For trypsinization, 16 μl of a 1:100 dilution (in 25 mM ammonium bicarbonate) of trypsin solution (V511C; Promega) was added, and the digests were incubated for 17 hr at 37° (1:37.5 trypsin/sample w/w). Following the trypsin digest, samples were acidified to pH 2 with 5 μl of 20% formic acid (JT Baker 0128-01) before desalting with C_{18} Desalting Tips (Rainin 17014047). Samples were eluted in 40 μl of a 50:50 acetonitrile (34851; Sigma): water (Fisher W5) mixture with 0.2% formic acid and then lyophilized. Samples were resuspended in 50 μl of 0.2% formic acid solution prior to mass spectrometry.

LC-MS/MS peptide sequencing was performed using the LTQ Orbitrap-XL mass spectrometer, ion source, UPLC system, EASY-Spray PepMap C_{18} column, and CID parameters for peptide fragmentation described above. Loading was performed at a 600 nl/min flow rate for 12 min, and then peptide separation was performed at a 300 nl/min flow rate over 63 min with a linear gradient of 2–30% (vol/vol) acetonitrile in 0.1% formic acid followed by a 2 min linear gradient from 30 to 50% acetonitrile. For MS/MS analysis, survey scans were recorded over a mass range of 325–1500 *m/z*. MS peak lists were generated with inhouse software called PAVA. Database searching was performed with Protein Prospector against the UniProtKB *C. albicans* database [SC5314, taxonomic identifier 237561; downloaded April 20, 2017 (last modified February 4, 2017) with 6153 entries]. The databases were concatenated with an equal number of fully randomized entries for estimation of the false-discovery rate (FDR). Database searching was carried out with tolerances of 20 ppm for parent ions and 0.8 Da for fragment ions. Peptide sequences were matched as tryptic peptides with up to two missed cleavages. Constant and variable modifications were set as described previously (O'Donoghue *et al.* 2012). The following Protein Prospector score thresholds were selected to yield a maximum protein FDR of <1%. A minimum "protein score" of 22 and a minimum "peptide score" of 15 were used; maximum expectation values of 0.01 for protein and 0.05 for peptide matches were used; "Report Homologous Proteins" was set to "Interesting." Only proteins with a minimum of two unique peptides for identification are reported.

Each protein's individual peptide (*i.e.*, spectral) counts from the three samples for a given strain were averaged, using a value of zero when no peptides were detected in a given sample. The percent abundance of a protein in a strain was calculated as the average spectral count from the three samples divided by the sum of the average spectral counts for all proteins detected in that strain. A complete list of proteins identified by these experiments are provided in File S4 in the supplemental material. We note that three proteins (Bgl2, Fet31, Rny11) appeared twice in the protein list for at least one sample; we have left both instances in place in File S4 and for the percent abundance calculations. Omitting the second entries of these proteins had less than a 0.1% effect on the abundance of all SAPs expect for the most highly expressed samples (Sap1, Sap3, Sap98, Sap99 in opaque

cells) where the largest effect was 0.66%; none of our conclusions are affected by the inclusion and/or exclusion of these entries.

Conditioned media BSA cleavage assays

In order to examine basal proteolytic activity, 3 ml SCD+aa+Uri cultures were started from white or opaque colonies and incubated for 24 hr at 25° on a roller drum. The pH of SCD+aa+Uri media, as evaluated by pH paper (Baker #4393-01 and #4391-01), decreased from ~5.0–5.5 to 3.0–3.5 during the 24 hr incubation, we note that this range is compatible with the reported pH preferences of much of the SAP family (Koelsch *et al.* 2000; Aoki *et al.* 2011). After the 24 hr incubation, supernatant was collected and filtered on a 0.45 μm PES filter (#725-2545; Thermo). BSA was added to the filtered supernatant at a final concentration of 0.5% (from a 20% stock solution) and the mixture was vortexed and incubated for 2 hr at 25° in a glass test tube on a roller drum. Samples were collected immediately after the addition of BSA and after 15, 60, and 120 min. The test tubes were vortexed prior to harvesting, and the harvested samples were mixed 1:4 with 8 M Urea, vortexed, and flash frozen in liquid nitrogen. Samples were run on 12.5% SDS-PAGE gels to evaluate effects on the full length BSA band. When indicated, pepstatin A (Sigma P5318) was diluted from 5 mM (in DMSO) to 1 mM (in DMSO) before being added to the filtered conditioned media (prior to addition of BSA) at a final concentration of 1 or 5 μM as indicated, equivalent volumes of DMSO were used as loading controls for these assays.

When screening the opaque transcriptional regulator knockout library, we processed 16 strains at a time and only harvested samples after 120 min. Candidates with reduced cleavage of BSA identified by the initial screen were subjected to further testing in order to control for experimental artifacts such as predominately white cell populations or lower culture densities. First, we repeated the assay while microscopically verifying the cell type of each culture. This eliminated the white cell population concern for all but two strains for which we could not get majority opaque populations (*bcr1*, *fgr15*). We then repeated the assay with the remaining candidates and, after verifying cell type, determined the cell density of each sample by flow cytometry. To compensate for the lower cell density observed for several strains after 24 hr, the assay was repeated with cultures incubated for 40 or 44 hr. After accounting for cell type and culture density, only the *efg1* and *wor3* deletions exhibited a BSA cleavage-deficient phenotype.

Flow cytometry proliferation and expression assays

Flow cytometry assays used either a BD Accuri C6 Plus (basic proliferation assays, GFP-based coculture assays) or a BD FACS Celesta (mCherry-based coculture and Proteinase K pretreatment reporter assays). The BD Accuri C6 Plus used a 488 nm laser with a 533/30 bandpass filter, samples were loaded from 96-well U-bottom plates (351177; Falcon), and normal acquisition was 10 μl of sample on the slow setting. The BD FACS Celesta used a 488 nm laser with a 530/30 bandpass filter and a 561 nm laser with a 610/20 bandpass filter, samples were loaded from 5 ml tubes (352052; Falcon) and normal acquisition was 10,000 events on the high setting.

For flow cytometry proliferation assays, SCD+aa+Uri overnight cultures (25°) were started from white or opaque colonies of each strain; independent cultures were processed in parallel for repeats of a given strain or condition. The following morning, cultures were diluted back to OD_{600} = 0.5 in 5 or 15 ml fresh SCD+aa+uri media and grown for 5–10 hr, depending on the assay, at 25° in a roller drum. Cells were then harvested, washed twice with 4 ml D-PBS, resuspended in SD+Uri, and diluted to OD_{600} = 0.5 in SD+Uri. Cell densities were verified by flow cytometry, and the cells were then diluted 1:10 to OD_{600} = 0.05 in the appropriate medium (*e.g.*, SD + BSA + Uri or SD + AmS + Uri) and gently vortexed. The density of each culture was then determined by flow cytometry, and the strains were grown on a roller drum at 25°. At each subsequent time point, cultures were gently vortexed, samples were removed, and denser samples were diluted with D-PBS prior to determining cell density by flow cytometry. Cell counts for proliferation assays were based on the number of cells detected in a 10 μl sample multiplied by the sample's dilution. For the assay comparing proliferation on different proteins (BSA, HSA, hemoglobin, myoglobin), the initial 10% protein stocks were dialyzed at 4° in 3500 MWCO Slide-A-Lyzer Dialysis Cassettes (#66330; Thermo) *vs.* distilled water for ~8 hr (roughly 1:250) and then against fresh distilled water for a further 16 hr (again, roughly 1:250) prior to incorporation into the medium. For the 37° BSA proliferation assay, samples were incubated in a 37°, rather than a 25°, roller drum and cells were harvested and plated for cell type determination as described in File S1. For the BSA as a carbon source assays, cells were diluted to OD_{600} = 0.5 in S + Uri and then 1:10 to OD_{600} = 0.05 in either S + BSA + Uri or S + BSA + AmS + Uri media.

Flow cytometry coculture proliferation assays: The coculture proliferation assays followed the protocol described above with the following modifications. After the D-PBS washes, SD+Uri resuspension, and OD_{600} determination, the two strains were mixed at defined Tagged/Untagged ratios (*e.g.*, 100/0, 50/50, 20/80, 5/95, and 0/100 for the wild type opaque and white experiments) where the two strains had a combined starting OD_{600} of 0.5. Expression of a Tef2-GFP fusion protein was used to distinguish strains, this reporter was expressed by the wild type opaque strain except in the cases of the wild type white cell Tef2-GFP: wild type opaque cell Tef2-mCherry fluorophore swap experiment, and the wild type white cell Tef2-GFP: opaque quintuple *SAP* deletion strain coculture experiment.

Flow cytometry mCherry reporter assays: The coculture mCherry reporter proliferation assays followed the protocol described above with the following modifications. After the D-PBS washes and SD+Uri resuspension, the initial dilution

in SD+Uri was to OD_{600} = 1.0, rather than 0.5, and the subsequent 1:10 dilution into the appropriate media was to OD_{600} = 0.1, rather than 0.05. Cells were analyzed using a BD FACS Celesta rather than a BD Accuri C6 Plus. The Tef2-GFP fusion protein was used to distinguish between the opaque cells (GFP positive) and the white strains expressing the mCherry reporters for *OPT1*, *OPT2*, *SAP2*, or *UGA4* expression (GFP negative). For the proteinase K pretreatment assays, 10 ml of a 10% BSA solution was incubated with 2.5 μl of proteinase K (NEB P8107S) for 30 min at room temperature (~22°). The proteinase K-treated BSA, in parallel with a mock treated BSA control, was then used to make SD+BSA+Uri media as described above.

Flow cytometry analysis: Data for each sample was exported as an FCS file, all subsequent analysis was done with R (R Core Team 2019) using the flowCore (Ellis *et al.* 2019), ggcyto (Van *et al.* 2018), and tidyverse (Wickham 2017) packages. For the myoglobin samples, which accumulated debris during the experiment, the data were filtered during analysis to exclude events with a FSC of <200,000. For the coculture experiments performed on the Accuri (Figure 7B and Supplemental Material, S10 and S12), data were first filtered to exclude those with no GFP fluorescence measurement. Cells were defined as GFP positive if the ratio of GFP.A/SSC.A was >0.04. For the coculture and/or reporter experiments performed on the Celesta (Figure 7C and Figure S11), cells were defined as GFP positive if the ratio of GFP.A/SSC.A was >0.5. In both sets of coculture analysis, the GFP positive evaluation was performed on all samples (including those that should contain 100% or 0% GFP positive cells).

Growth rates were calculated using a sliding window approach; the natural log of cell count was regressed against time for each set of five time points based on previously reported protocols (Ziv *et al.* 2013). The growth rate was calculated as the greatest slope of a regression that had both an R^2 >0.9 and at least a fourfold change over the five time points. Subsequently, lag duration was estimated as the intersection of this regression with a horizontal line determined by the cell count at the first time point. Confidence intervals for mean growth rate and lag duration were calculated as ±1.96 the SEM. Growth rates calculated based on Flow Cytometry Proliferation Assays are included in File S5.

White-opaque switching assay and variants

The white-to-opaque and opaque-to-white switching assays evaluating the effect of *SAP* deletions on switching rates followed previously reported protocols (Miller and Johnson 2002; Zordan *et al.* 2007; Lohse *et al.* 2016). Details about this method, the modifications to evaluate white-opaque switching when BSA is the sole nitrogen source, and the modifications to evaluate the effect of BSA on opaque cell stability at 37° are addressed in the Supplemental Materials and Methods (File S1).

NanoString transcriptional profiling

Transcriptional analysis was conducted using NanoString probes against a set of 59 *C. albicans* genes (one probe per gene). Probes were designed and synthesized by NanoString Technologies. A list of target genes and probe sequences can be found in File S6.

Overnight cultures of strains being profiled were grown in SD+AmS+Uri at 25°; in the morning, cells were diluted to a density of 5×10^6 cells/ml (opaque cells), 2.5×10^6 cells/ml (white cells), or 1×10^7 cells/ml (2 hr experiments) in the desired media. Ammonium sulfate samples were harvested 8 hr postdilution, other samples were harvested 2 hr postdilution or when cells were growing logarithmically, as indicated. Cells were pelleted, frozen in liquid nitrogen, and stored at −80° pending further processing. Total RNA was extracted using a MasterPure Yeast RNA Purification Kit (MPY03100; Lucigen), the RNA concentration was determined on a Nanodrop 2000C (Thermo Scientific), and RNA quantity was normalized to 400 ng per sample. Samples were processed on a nCounter Sprint Profiler (NanoString Technologies) at the Center for Advanced Technology at the University of California, San Francisco. Read count data were processed using the nSolver analysis software (NanoString Technologies). Two replicates were analyzed for each sample except for wild-type opaque cells when BSA was the sole source of nitrogen; in this case, four replicates were analyzed.

Raw counts were exported and then analyzed with R (R Core Team 2019) using the tidyverse package (Wickham 2017). All data were normalized based on four housekeeping genes (*PGA59*, MTL*a1*, *TBP1*, *HTA1*) whose average expression spans almost three orders of magnitude. The geometric mean of these four housekeeping genes for each sample was calculated (*PGA59*, 11,5; MTL*a1*, 5.84; *TBP1*, 7.59; *HTA1*, 9.6), and the difference between the geometric mean of these housekeeping genes across all samples and the geometric mean of these four housekeeping genes in each individual sample was determined. This difference was then subtracted from all reads in that individual sample to normalize the data, and these normalized read counts were used for all further comparisons and analyses. Student's *t*-tests were performed on log transformed expression data to compare between the ammonium sulfate and BSA conditions for wild type opaque and white cells either logarithmically growing or at the 2 hr time point (Figure S3). Significance was evaluated using a 5% FDR (Benjamini–Hochberg procedure). Raw and normalized NanoString transcriptional data can be found in File S6.

Optical density proliferation assays

The optical density proliferation assays modified our previously reported protocol (Lohse *et al.* 2016) to account for the increased delay before proliferation when BSA was the sole nitrogen source. This method is described in detail in the Supplemental Materials and Methods (File S1).

Data availability

The authors state that all data necessary for confirming the conclusions presented in the article are represented fully within the article, including Supplemental Material. Strains and plasmids are available upon request. All Supplemental Items have been uploaded to the GSA Figshare portal. Supplemental Materials and Methods and Results as well as legends for all supplemental items are included in File S1. A complete list of media, oligonucleotides, plasmids, and strains used in this study can be found in File S2. Additional data for MSP-MS experiments can be found in Figure S1 and File S3. Additional data for proteomics experiments can be found in Table S1 and File S4. Additional data for BSA cleavage assays can be found in Figures S1, S6, and S8. Additional data for cell type switching experiments can be found in Tables S2 and S3. Additional data for flow cytometry based proliferation experiments can be found in Figures S2, S8, S10, S11, and S12 as well as File S5. Additional data for transcriptional profiling experiments can be found in Figures S3, S4, S5, S7, and S9 as well as File S6. Additional data for optical density based proliferation experiments can be found in Figures S6 and S8 as well as File S7.

All raw spectrum (.RAW) files from the MSP-MS and proteomics experiments reported in this study are available for download from the MassIVE resource (https://massive.ucsd.edu/ProteoSAFe/static/massive.jsp), numbers MSV000085279 (MSP-MS) and MSV000085283 (proteomics). Supplemental material is available at figshare: https://doi.org/10.25386/genetics.12818894.

Results

Opaque cells secrete more proteolytic activity than white cells

To assess secreted proteolytic activity using a global approach, we profiled conditioned media using the MSP-MS assay (O'Donoghue *et al.* 2012). In brief, white or opaque cell conditioned media were incubated with a library of 228 synthetic 14-mer peptides, and the resulting cleavage products (at 15, 60, and 240 min) were identified by liquid chromatography-tandem mass spectrometry (LC-MS/MS). We note that these experiments were performed with cells grown in medium containing ammonium sulfate; as such, these results reflect the "basal" activity of proteases rather than the activities induced when proteins are provided as the sole nitrogen source.

Opaque cell conditioned media exhibited higher proteolytic activity at each time point examined based on the number of unique cleavage events (377 opaque *vs.* 214 white cleavages after 60 min at pH 5.5) (Figure 1, B and C and File S3). In general, cleavages observed in white cell conditioned media were also observed in opaque cells (between 67% and 80%), while a majority of opaque cell cleavages (between 47 and 69%) are specific to opaque cell conditioned media (Figure S1A and File S3). Furthermore, we observed between 1.8- and 3.0-fold higher proteolytic activity at pH 5.5 than at pH 7.4, consistent with the reported preference of certain SAPs for acidic conditions (Koelsch *et al.* 2000; Aoki *et al.* 2011) (Figure 1B and Figure S1A).

To determine global protease substrate specificities, we generated iceLogo (Colaert *et al.* 2009) representations of the MSP-MS data. The iceLogos incorporate both cleaved and uncleaved positions in the peptide library to display enrichment for or against specific amino acids within four positions of the cleavage site (P4 to P4′, with cleavage occurring between P1 and P1′). At the 60 min time point, many features are shared between the white and opaque cleavage profiles. For example, there is an enrichment for hydrophobic (norleucine, phenylalanine, tyrosine) and positively charged (lysine, arginine) residues at the P1 positions (Figure 1D). Despite these broad similarities in cleavage preferences, there are several noticeable differences between the two cleavage profiles. For example, opaque cells show a preference (relative to white cells) for glycine at P4, valine at P2, and leucine at P1 (Figure 1D). Both the white and opaque conditioned media show certain specificity preferences that are characteristic of recombinantly produced Sap5 and Sap6 (which are normally expressed in *C. albicans* biofilms) (Winter *et al.* 2016), and, given the similarity among the *SAP* gene sequences (Parra-Ortega *et al.* 2009), it is likely that the MSP-MS data from both cell types are dominated by secreted SAP proteins.

We also collected cell-free conditioned media from white and opaque cells, added BSA, and evaluated BSA cleavage over the course of 2 hr. In agreement with the overall increased proteolytic activity observed in the MSP-MS assay, opaque cell conditioned media cleaved most of the BSA within 15 min and multiple cleavage products were observed by 2 hr (Figure S1B). White cell conditioned media, on the other hand, cleaved only a small fraction of the BSA to generate a single predominant cleavage product by 2 hr (Figure S1B).

Opaque cells secrete different SAPs than white cells

To relate the proteolytic activities of the two cell types to specific proteases, we performed shotgun proteomic analyses on white and opaque cell conditioned media (from cells grown on media containing ammonium sulfate) from three switching-capable strain backgrounds [SC5314, L26, and P37005 (Lockhart *et al.* 2002)] (File S4). Nine unique SAPs were detected in this experiment (Tables 1 and Table S1). On average, SAPs comprised 8% of peptides detected in white cell conditioned media and 48% of peptides detected in opaque cell conditioned media (Table 1). In absolute terms, opaque cells secreted around five times the amount of SAPs as white cells. Consistent with previous transcriptional profiling (Hube *et al.* 1994; White and Agabian 1995), Sap2 was the most abundant SAP secreted by white cells, at 4% of detected peptides (Table 1). For opaque cells, Sap1 was the most abundant SAP, at 17% of detected peptides (Table 1). Sap99 and Sap3 were also abundant in opaque cells, comprising 16 and 8% of detected peptides, respectively (Table 1).

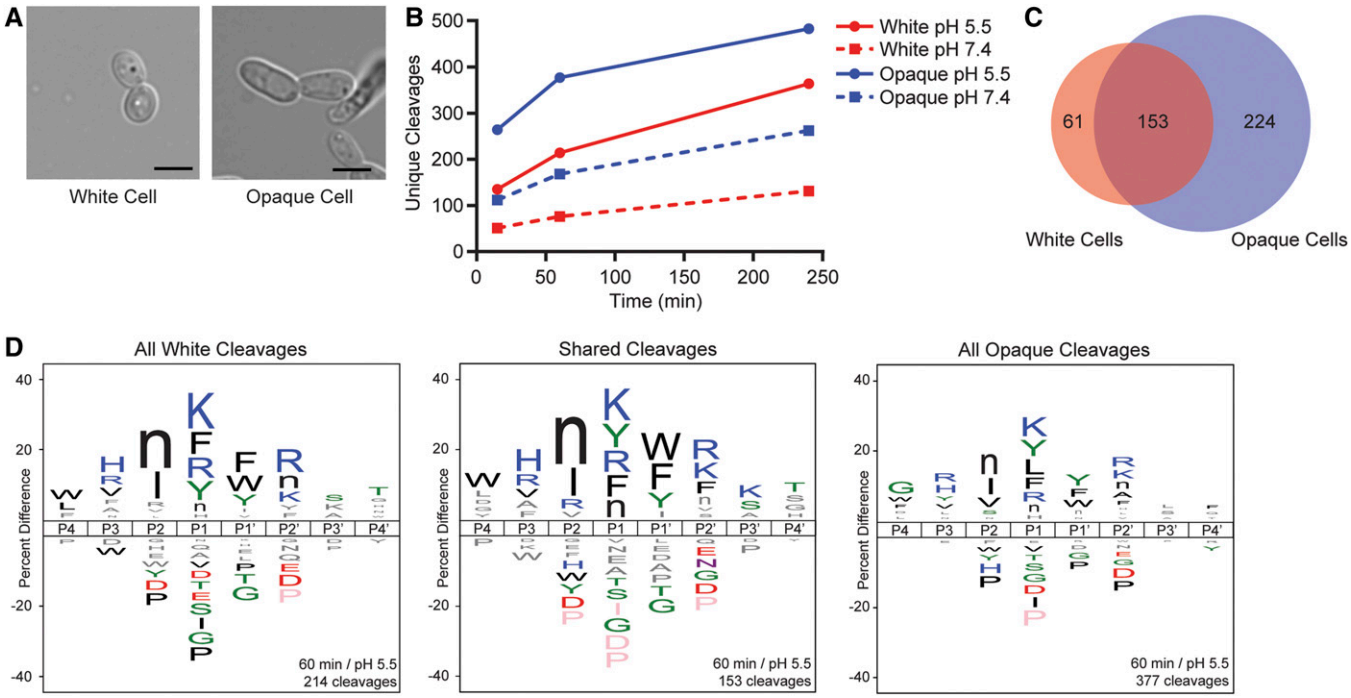

Figure 1 Opaque cells secrete higher and more diverse proteolytic activity than white cells. (A) Images of typical white (left) and opaque (right) *C. albicans* cells grown in liquid SCD+aa+Uri media at 25°. Bar, 5 μm, panel adapted from Lohse and Johnson (2016). (B) Comparison of the number of unique 8-mer cleavages seen in white (red) and opaque (blue) cell conditioned media at pH 5.5 (solid lines, circles) and pH 7.4 (dashed lines, squares) after 15, 60, and 240 min. (C) Quantification of the number of unique 8-mer cleavages common to both cell types or specific to one cell type (pH 5.5, 60 min). (D) iceLogo substrate specificity representation for 60 min conditioned media from white and opaque cells as well as for the cleavages shared by the two cell types. Colored residues indicate $P \leq 0.05$, gray residues indicate $0.05 < P \leq 0.3$, and "*n*" represents norleucine. Experiments in panels B–D were performed on conditioned media from cells grown in media containing ammonium sulfate; as such, these results reflect basal, rather than protein induced, proteolytic activity levels. All MSP-MS cleavages are compiled in File S3.

Also consistent with the previous transcriptional profiling (Hube *et al.* 1994; White and Agabian 1995; Lan *et al.* 2002; Tuch *et al.* 2010; Hernday *et al.* 2013), these three proteases each comprised <1% of the peptides detected in white cell conditioned media (Table 1). Likewise, the most abundant white cell SAPs (Sap2 and Sap7) were present at <1% of secreted peptides from opaque cells (Table 1). These results show that opaque cells secrete higher absolute levels of SAPs than do white cells, and that the SAP profiles are markedly different between the two cell types.

Putting aside the SAPs, we detected an average of 57 different proteins in opaque cell conditioned media (between 44 and 71 per strain) and an average of 77 different proteins in white cell conditioned media (between 73 and 83 per strain). With a few exceptions (*e.g.*, Sap7 and the phospholipase Plb4.5 in white cells, Sap98 and the acid phosphatase Pho112 in opaque cells), the most abundant proteins secreted by one cell type were detected, albeit at reduced levels, in the other cell type's conditioned media.

Opaque cells are more efficient at using proteins as a sole nitrogen source

Soll and colleagues previously reported that opaque cells from the WO-1 strain proliferate sooner (that is, there is a shorter delay after inoculation before they begin logarithmic proliferation) than white cells when BSA is the sole nitrogen source (Srikantha *et al.* 1995; Kvaal *et al.* 1999). Consistent with this result, we found that opaque cells from the three strain backgrounds used in this study began logarithmic growth sooner than white cells when BSA was the only source of nitrogen (roughly 18–24 *vs.* 72–120 hr, depending on starting cell density and nutrient carry over from dilutions) (Figure 2A). We also observed that opaque cells reach a slightly higher maximum proliferation rate, doubling in slightly <4 hr as opposed to every 5 hr for white cells (File S5). The presence of BSA does not appear to increase white-opaque switching in either direction relative to rates on ammonium sulfate and does not block temperature (37°) induced *en masse* opaque-to-white switching (SI Results, Figure S2, A and B and Table S2).

To determine whether similar proliferation differences were observed with proteins other than BSA, we measured proliferation on human serum albumin (HSA), hemoglobin, and myoglobin. Opaque cells began proliferating at 30–40 hr when HSA was the nitrogen source compared with no growth after 90 hr for white cells (Figure 2B). Opaque cells also began proliferating sooner and slightly faster than white cells when hemoglobin was the sole nitrogen source, although the difference between the two cell types was less pronounced than with BSA (proliferation after 8–16 *vs.* 20–40 hr, doubling

Table 1 Average total basal Sap abundance

Protein	Average percent of total counts, all white strains	SD percent of total counts, all white strains	Average percent of total counts, all opaque strains	SD percent of total counts, all opaque strains
Sap1	0.42	0.03	17.36	2.21
Sap2	3.61	2.07	0.49	0.23
Sap3	0.51	0.23	8.37	0.64
Sap7	1.85	0.55	0.00	0.00
Sap8	0.14	0.10	0.82	0.59
Sap9	0.50	0.06	0.04	0.05
Sap10	0.85	0.27	0.26	0.03
Sap98	0.00	0.00	4.21	2.57
Sap99	0.57	0.18	16.09	6.33
All Saps	8.44	2.58	47.64	9.90

The total abundance of all Saps detected in white and/or opaque cells averaged across three *C. albicans* strain backgrounds (L26, P37005, SC5314). Sap4, Sap5, and Sap6, which are normally associated with biofilms, were not detected in any sample of either cell type. These experiments were performed on conditioned media from cells grown in media containing ammonium sulfate; as such, these results reflect basal, rather than protein induced, levels of these proteins.

roughly every 2 hr as opposed to 3 hr) (Figure 2B and File S5). In contrast to the other protein sources, myoglobin seemed equally well utilized by white and opaque cells as both cell types rapidly began to proliferate, although opaque cells still proliferated slightly faster (doubling every 3.5 *vs.* 5 hr) (Figure 2B and File S5). These results suggest that opaque cells are generally more efficient than white cells at utilizing proteins as a nitrogen source, but that protein-specific characteristics (*e.g.*, primary sequence, protein size, and/or folding) affect the difference with which the two cell types can utilize proteins.

C. albicans is unusual among fungi in that it can utilize free amino acids as a carbon source in addition to their more common utilization as a nitrogen source (Vylkova *et al.* 2011; Priest and Lorenz 2015; Ene *et al.* 2016). To determine whether proteins could be used as a sole carbon source, we examined the proliferation of both cell types on minimal media containing BSA but lacking glucose (both with and without ammonium sulfate). Neither white nor opaque cells reached their typical final cell density (roughly 10^8 cell/ml) in these conditions (Figure S2C), indicating that *C. albicans*, although it can utilize proteins as a nitrogen source, cannot efficiently use proteins, at least across the scope of this experiment, as their sole carbon source.

White and opaque cells express different SAPs in response to nitrogen source

To understand the response of white and opaque cells to different nitrogen sources, we used NanoString probes to measure expression of the *SAP* family genes, 13 transporters (8 *OPT*s, 2 *PTR*s, 2 ammonium permeases, and 1 amino acid permease), and 33 additional genes (59 genes total) on ammonium sulfate, BSA, myoglobin, and hemoglobin, as sole nitrogen sources, as well as nitrogen-depleted medium (Figure 3A). To allow for an equivalent comparison between cell types on BSA, we profiled both cell types on BSA (1) after 2 hr in the new medium and (2) when they began logarithmic proliferation (~24 hr for opaque cells, ~96 hr for white cells).

"Basal" expression is observed in ammonium sulfate: We first consider proliferation on ammonium sulfate, which we consider to be the "basal" (*i.e.*, nitrogen-replete) expression program (as opposed to the "induced" expression program described below which depends on protein as the sole nitrogen source). Consistent with previous reports (Hube *et al.* 1994; White and Agabian 1995; Lan *et al.* 2002; Tuch *et al.* 2010; Hernday *et al.* 2013), white cells (relative to opaque cells on the same medium) express higher levels of the oligopeptide transporters *OPT1* (8-fold), *OPT3* (40-fold), *OPT7* (14-fold), and *PTR22* (6-fold) (Figure 3B left panel, File S6). Although Sap2 was detected in white cell conditioned media in the proteomics experiments discussed above, *SAP2* transcript levels were similarly low in both white and opaque cells growing on ammonium sulfate. In agreement with the proteomics experiments, opaque cells in ammonium sulfate express higher levels of *SAP1* (160-fold), *SAP3* (5.9-fold), *SAP99* (15-fold), and the oligopeptide transporter *OPT4* (65-fold) relative to white cells in the same medium (Figure 3B left panel, File S6).

"Induced" expression is observed when protein is the sole nitrogen source: In contrast to the "basal" expression profiles observed in ammonium sulfate, the "induced" response is observed when BSA is provided as the sole nitrogen source. On such media (relative to ammonium sulfate), we observe (1) groups of genes that are upregulated in both cell types, including *SAP2* (1450-fold in white cells, 420-fold in opaque cells), *SAP3* (18-fold in white cells, 630-fold in opaque cells), *OPT2* (70-fold in white cells, 210-fold in opaque cells), *OPT5* (170-fold in white cells, 230-fold in opaque cells), and *PTR2* (120-fold in white cells, 580-fold in opaque cells), (2) genes that are upregulated only in white cells including *OPT1* (15-fold), and (3) genes that are only upregulated in opaque cells including *SAP1* (fivefold), *SAP8* (900-fold), and *OPT7* (19-fold) (Figures 3, B and C right panel, Figure S3, and File S6). The opaque cell "induced" response is not simply an upregulation of the basal pattern; for example, neither *OPT4* nor *SAP99* are induced. Although the white and opaque cell

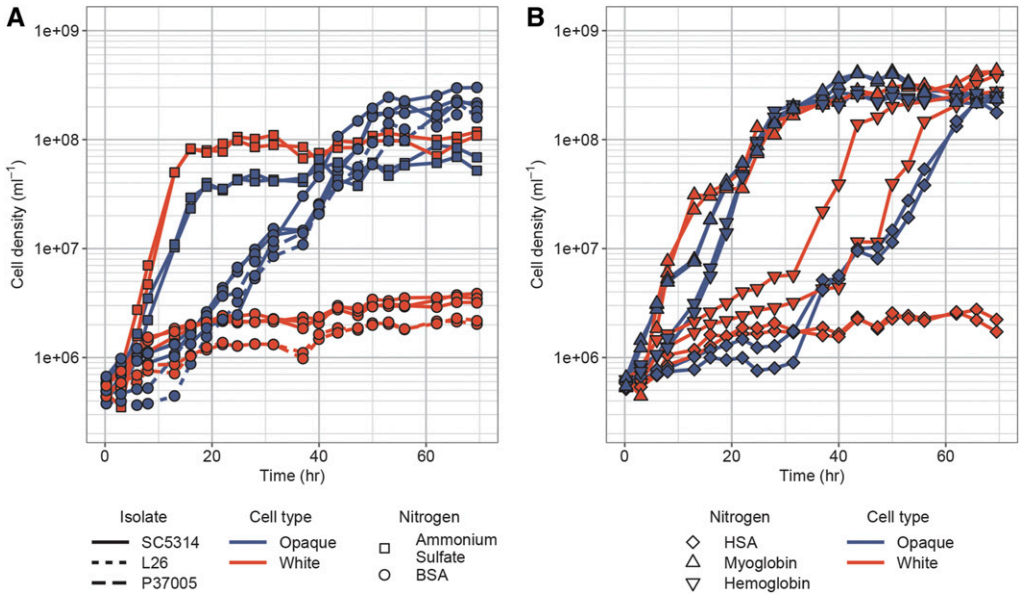

Figure 2 Opaque cells are more efficient than white cells at utilizing protein as the sole nitrogen source. (A) Proliferation of white (red) and opaque (blue) cells from three backgrounds (SC5314, solid line; L26, short dash; P37005, long dash) when ammonium sulfate (squares) or BSA (circles) is the sole nitrogen source. (B) Proliferation of white (red) and opaque (blue) cells from the SC5314 background when HSA (diamonds), myoglobin (upward triangles), or hemoglobin (downward triangles) is the sole nitrogen source. Cell counts in both panels were determined by flow cytometry.

induced responses share several genes, the magnitude of induction of these genes can vary greatly and is usually much greater in opaque cells; for example, *SAP3* and *PTR2* transcripts are present at ~200- and 16-fold higher levels in "induced" opaque cells (File S6).

Both cell types' responses to BSA as the sole nitrogen source are similar to their responses when either hemoglobin or myoglobin are the sole nitrogen source (Figure 4A and File S6). Specifically, opaque cells upregulate *SAP1*, *SAP2*, *SAP3*, *SAP8*, *OPT2*, *OPT5*, *OPT7*, and *PTR2* at least fivefold (Figure 4A left panel, File S6) while white cells upregulate *SAP2*, *SAP3*, *OPT2*, *OPT5*, and *PTR2* at least fivefold regardless of whether BSA, hemoglobin, or myoglobin is provided as the sole nitrogen source (Figure 4A right panel, File S6). A few other genes are upregulated specifically on myoglobin or hemoglobin, but the magnitude is lower than seen for genes upregulated in response to all three proteins (Figure S4, A and B and File S6).

Initial responses to protein and nitrogen starvation: We also measured the transcriptional response of white and opaque cells before they had a chance to adapt to proteins as their sole nitrogen source (2 hr postinoculation in BSA) and to simple nitrogen starvation (2 hr postinoculation) (SI Results, Figure 4B, Figures S4C and S5, and File S6). White cells had a limited transcriptional response to either of these conditions, with expression of a small number of genes changing in both conditions (*OPT2* and *UGA4* upregulated, *OPT7* downregulated), and expression of a few other genes changing in only one of the two conditions (*e.g.*, *SAP2* upregulated in response to nitrogen starvation) (Figure 4B right panel, Figures S4C and S5 and File S6). In contrast, opaque cells exhibited a broader and higher magnitude transcriptional response to both conditions, upregulating a number of genes (including *OPT2*, *OPT5*, *PTR2*, and *UGA4*) and downregulating *OPT7* (Figure 4B left panel, Figures S4C and S5 and File S6).

If we compare opaque cells acutely starved for nitrogen for 2 hr with their later adaptation to BSA as the sole nitrogen source, we find two major differences: (1) the greater magnitude of *SAP* upregulation during growth on BSA and (2) the loss of the upregulation of *UGA4* and other genes observed under acute (2 hr) nitrogen starvation. Based on these observations, we hypothesize that opaque cells mount an initial response to nitrogen starvation that gradually dissipates as they begin to upregulate the *SAP*s allowing them to utilize proteins (Figure 3D).

Several general points emerge from this transcriptional analysis. First, white and opaque cells differ in their basal expression of the *SAP*s and *OPT*s, that is, their expression of these genes in nitrogen replete medium (Figure 3D). Superimposed on these distinct basal expression patterns are the induction of different sets of *SAP*s and *OPT*s in response to the presence of protein as the sole nitrogen source. In opaque cells, some of the basal opaque-specific genes are further upregulated, and a series of new genes are activated, giving an induced expression pattern that is markedly different, both in terms of genes involved as well as the magnitudes of induction, from that of white cells (Figure 3D).

Contributions of individual SAPs

The aspartyl protease active site inhibitor pepstatin A blocked both basal opaque BSA cleavage (Figure S6A) and opaque cell proliferation on BSA as the sole nitrogen source at concentrations that did not affect proliferation on ammonium sulfate (Figure S6B). These results indicate that both BSA cleavage and growth are dependent on *SAP* protease activity. To identify the specific *SAP*(s) responsible, we examined basal opaque BSA cleavage and opaque cell proliferation on BSA in a set of strains where combinations of either four or five of the

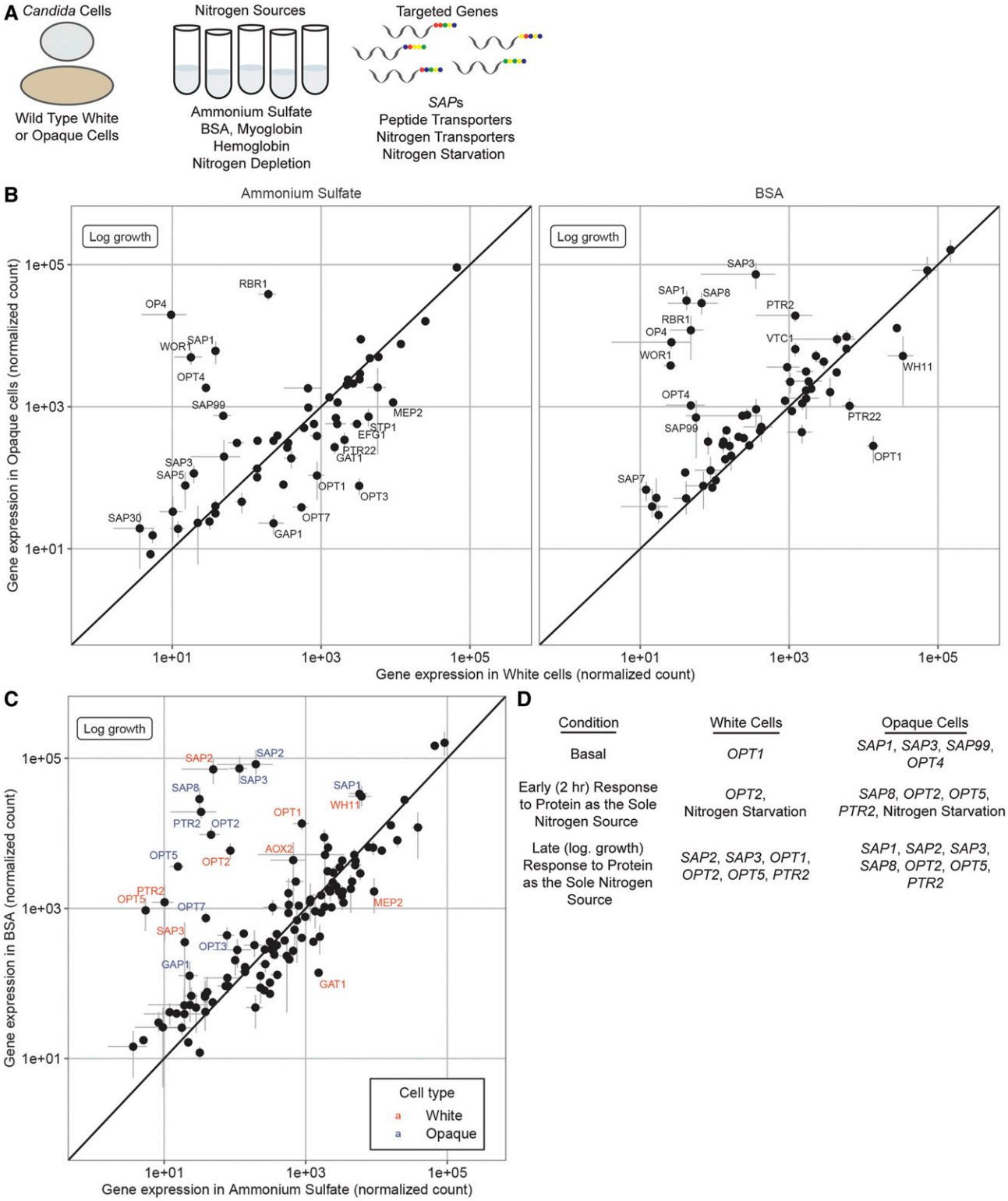

Figure 3 White and opaque cells express different *SAP*s and peptide transporters in response to different nitrogen sources. (A) NanoString probes were used to measure expression of the *SAP* family, transporters, and genes associated with nitrogen starvation. (B) White (lower right) and opaque (upper left) enrichment of selected genes in cells undergoing logarithmic proliferation on ammonium sulfate (left chart) or BSA (right chart) as the sole nitrogen source. Names are indicated for genes differentially regulated at least fivefold between cell types, the line ($y = x$) indicates equal expression in both cell types. (C) Enrichment of selected genes in cells undergoing logarithmic proliferation on ammonium sulfate (lower right) or BSA (upper left) as the sole nitrogen source. Names are indicated for genes differentially regulated at least fivefold between the two nitrogen sources in white (red) and opaque (blue) cells, the line ($y = x$) indicates equal expression on both nitrogen sources. In B and C, lines extending from points show the range between replicates, if no lines are visible the range is smaller than the point. (D) Summary of *SAP*s and transporters that are basally expressed and/or expressed when extracellular proteins are the sole nitrogen source.

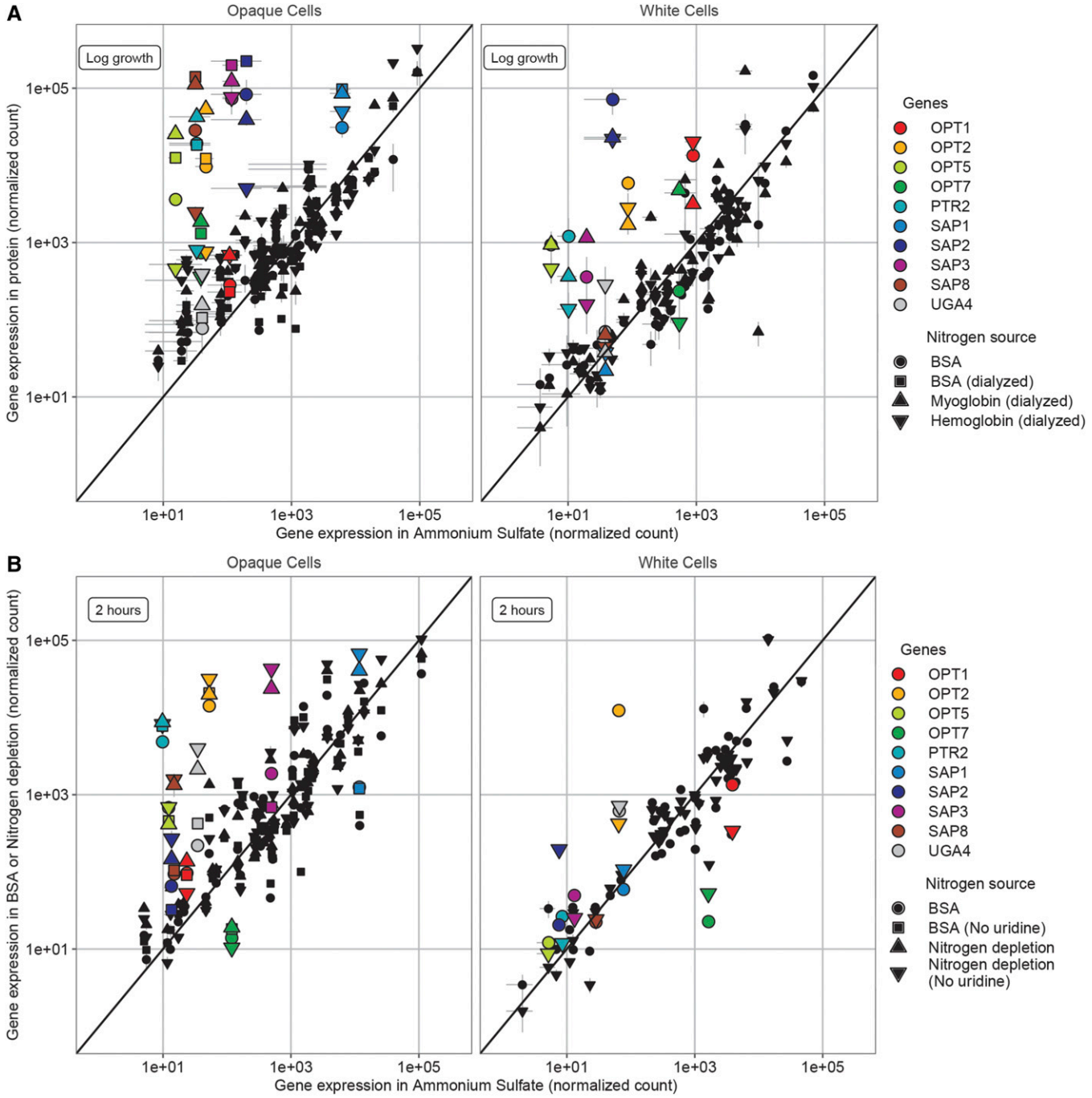

Figure 4 Transcriptional response of white and opaque cells to different proteins as the sole nitrogen source and nitrogen starvation. (A) Enrichment of selected genes in opaque (left) or white (right) cells undergoing logarithmic proliferation on different proteins as the sole nitrogen source (*y*-axis) plotted relative to cells growing when ammonium sulfate is the sole nitrogen source (*x*-axis). BSA (circles), dialyzed BSA (squares), myoglobin (upward facing triangles), and hemoglobin (downward facing triangles) are the three proteins used as the sole nitrogen sources, the line ($y = x$) indicates equal expression on both protein and ammonium sulfate. (B) Enrichment of selected genes in opaque (left) or white (right) cells after 2 hr exposure to media with BSA and trace uridine (circles), BSA without uridine (squares), no nitrogen with trace uridine (upward facing triangles), or no nitrogen without uridine (downward facing triangles) as the sole nitrogen source(s) (*y*-axis) plotted relative to cells growing when ammonium sulfate is the sole nitrogen source (*x*-axis). In both panels, lines extending from points show the range between replicates; if no lines are visible the range is smaller than the point.

opaque-expressed *SAP*s (*SAP1*, *SAP2*, *SAP3*, *SAP8*, and *SAP99*) were deleted. We found that basal opaque BSA cleavage was abolished when all five of these *SAP*s were deleted (Figure S6C). When four of the five SAPs were deleted, we found that the presence of either *SAP1* or *SAP3* (both of which are basally expressed in opaque cells and were detected in our proteomic analysis) could maintain basal BSA cleavage at near wild type levels but that *SAP2*, *SAP8*, or

SAP99 alone did not support cleavage (Figure S6C). As *SAP2* and *SAP8* are not basally expressed by opaque cells, their inability to support BSA cleavage is not unexpected; however, the inability of *SAP99* to support opaque BSA cleavage was a surprise as *SAP99* is basally expressed and was detected in the proteomic analysis.

Efficient opaque cell proliferation on BSA as a sole nitrogen source was abolished (for at least 7 days, the extent of the experiment) when all five *SAP*s were deleted (Figure 5). The presence of either *SAP1*, *SAP2*, *SAP3*, or *SAP8*, but not *SAP99*, was sufficient to allow opaque cell proliferation on BSA, although this proliferation was delayed relative to the wild type strain (Figure 5 and File S5). This result is consistent with our transcriptional profiling in that all four of the *SAP*s (*SAP1*, *SAP2*, *SAP3*, and *SAP8*) that supported growth are highly induced. We note that the delay before opaque cells begin to proliferate when BSA is the sole nitrogen source is longer (by 15–35 hr) when only one *SAP* gene is present, but, once they begin, the proliferation rates were slightly faster than the parental strain (doubling times of roughly 3.2–3.3 hr *vs.* 3.8 hr) (File S5). We believe that the delay before active proliferation (henceforth referred to as "lag") reflects the time it takes to produce sufficient BSA cleavage products at a rate needed for logarithmic growth.

We did not observe significant changes in the basal expression of *SAP4-SAP7*, *SAP9*, *SAP10*, or *SAP30* when *SAP1*, *SAP2*, *SAP3*, *SAP8*, and *SAP99* were deleted (Figure S7 and File S6), suggesting that there is no compensatory upregulation in response to the loss of basal opaque cell *SAP* expression. The only exception was an increase in *SAP98* expression when *SAP99* was deleted, but these two genes are adjacent and we believe that this upregulation is likely the result of the nearby genetic manipulation. As *SAP98* does not appear to contribute to growth on BSA as a nitrogen source (a number of deletion strains containing it failed to cleave BSA or proliferate), we do not consider it further. Finally, we note that deletions of either four or five of the opaque-expressed *SAP*s (*SAP1*, *SAP2*, *SAP3*, *SAP8*, and *SAP99*) do not appear to block or increase white-opaque switching in either direction (Table S3, SI Results, File S1).

Control of opaque cell basal proteolytic activity

To identify regulators controlling opaque cells' basal proteolytic activity, we screened a library of 188 opaque transcription regulator deletion strains (Lohse *et al.* 2016) for loss of BSA cleavage in conditioned media. Only 2 of the 188 opaque strains tested, the *efg1* and *wor3* deletions, lacked basal opaque cell proteolytic activity as monitored by BSA cleavage (Figure S8A). Both Efg1 and Wor3 are known regulators of white-opaque switching and both are required for full expression of the opaque cell transcriptional program (Sonneborn *et al.* 1999; Zordan *et al.* 2007; Hernday *et al.* 2013; Lohse *et al.* 2013). In addition, Efg1 has previously been linked to *SAP* expression in the oral epithelial cell and parenchymal organ invasion models, although these experiments were conducted with white cells (Felk *et al.* 2002; Korting *et al.* 2003). Because *WOR3* expression in opaque cells is dependent on the presence of Efg1 (Hernday *et al.* 2013), the most parsimonious explanation for the *efg1* phenotype is that it reflects the loss of *WOR3* expression rather than a Wor3-independent mechanism.

To understand the roles of Efg1 and Wor3 in expressing basal opaque cell proteolytic activity, we used NanoString probes to profile expression of the *wor3* and *efg1* deletion strains proliferating in ammonium sulfate. Consistent with the BSA cleavage results, we observed that expression of the basal opaque program (defined by upregulation of *SAP1*, *SAP3*, *SAP99*, and *OPT4* relative to white cells in the same medium) was lost in both the opaque *wor3* and *efg1* deletion strains (Figure 6A lanes 1–3, File S6). In contrast, deletion of *STP1* or *CSR1* (which contribute to the opaque cell response to proteins as the sole nitrogen source as described below), affected neither basal opaque proteolytic activity nor expression of the basal opaque program (Figure 6A lanes 1, 4–5, Figure S8A, File S6). These results differ from white cells, where the *stp1* deletion strain affected basal white cell expression of *OPT1* and *SAP2*, consistent with previous reports (Martínez and Ljungdahl 2005). The *csr1*, *efg1*, and *wor3* deletions, on the other hand, had minimal or no effect on basal white cell expression of *OPT1* or *SAP2* (Figure 6B, lanes 1–5, File S6).

Regulation of the opaque cell response to protein as the sole nitrogen source

To identify regulators controlling opaque cells' ability to use proteins as a nitrogen source (which requires the induced response), we screened the aforementioned library of 188 opaque transcription regulator deletion strains (Lohse *et al.* 2016) for failure to proliferate when BSA was the sole nitrogen source. In this screen, only the *stp1* deletion strain showed a pronounced proliferation defect, with no detectable growth after 3 days. This result is consistent with previous reports that Stp1 was necessary for white cell proliferation on BSA (Martínez and Ljungdahl 2005). The *csr1*, *efg1*, and *wor3* deletion strains exhibited milder defects, showing either late and/or slow proliferation relative to wild type (Figure S8B, File S1, S5, and S7).

In order to understand the relationships among Stp1, Csr1, Efg1, and Wor3 in opaque cells, we used NanoString probes to profile expression of logarithmically proliferating opaque *csr1*, *efg1*, *stp1*, and *wor3* deletion strains when BSA is the sole nitrogen source. Expression of *SAP1*, *SAP2*, and *SAP3* was reduced between 18- and 330-fold (relative to wild type) when *EFG1* or *WOR3* were deleted and expression of *SAP2*, *SAP3*, and *SAP8* was reduced between 5- and 25-fold (relative to wild type) when *CSR1* was deleted (Figure 6A lanes 6–9, File S6). Deletion of *CSR1*, *EFG1*, or *WOR3* had minimal effect on the expression of the transporters *OPT2*, *OPT5*, *OPT7*, or *PTR2* under these conditions (Figure 6A lanes 6–9, File S6). We interpret these results to indicate that Efg1 and Wor3 are important for the upregulation of *SAP1*, *SAP2*, and *SAP3*, while Csr1 is important for the upregulation of

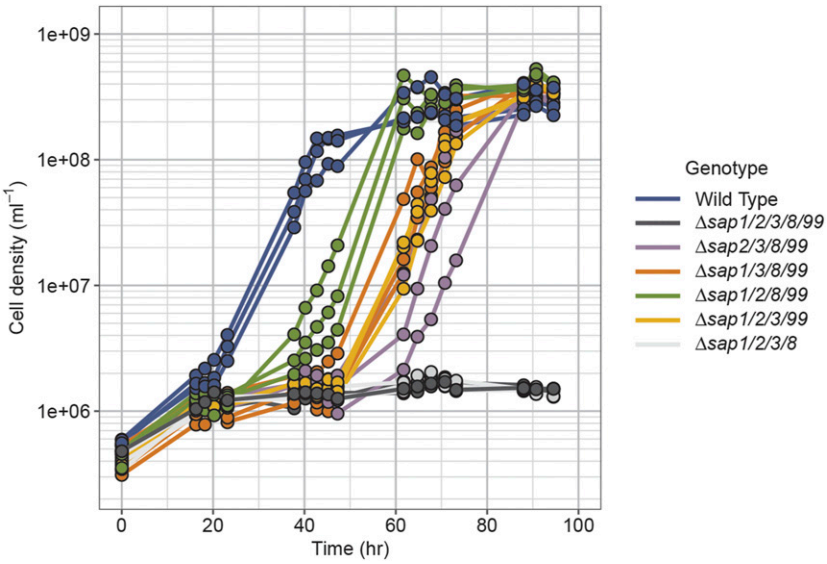

Figure 5 Any one of four *SAP* genes (*SAP1*, *SAP2*, *SAP3*, *SAP8*) is sufficient for opaque cell proliferation when BSA is the sole nitrogen source. Proliferation of opaque strains with combinations of either four or five of the five opaque-expressed *SAP*s (*SAP1*, *SAP2*, *SAP3*, *SAP8*, and *SAP99*) deleted on media where BSA is the sole nitrogen source. Cell counts were determined by flow cytometry.

SAP2, *SAP3*, and *SAP8*. Our results indicate that neither Csr1, Efg1, nor Wor3 contribute to the upregulation of peptide transporters (Figure 6C, File S6).

The *stp1* deletion strain had a more pronounced defect. Opaque cells deleted for *STP1* will eventually proliferate on BSA as a sole nitrogen source, but this proliferation is delayed (starting after 3–4 days *vs.* 1 day for the parental strain), and, once begun, slow (doubling every 17.5 hr *vs.* 4 hr for the parental strain) (Figure S8B and File S5). Under these conditions, the induced response of most of the SAPs and transporters (*SAP2*, *SAP8*, *OPT2*, *OPT5*, *PTR2* and, to a lesser extent, *SAP3*) was largely missing (Figure 6A lanes 6 and 10, File S6). In contrast, *SAP1* and *SAP99* were expressed at higher levels (Figure 6A lanes 6 and 10, File S6), but, despite this compensation, overall *SAP* transcript levels are down almost twofold (113K *vs.* 217K, File S6). These results show that most of the response of opaque cells to protein as the sole nitrogen source is dependent on Stp1. Consistent with these results, we also observed a decreased response of the *stp1* opaque cell deletion to acute (2 hr) nitrogen starvation (Figure S9 lanes 3–6, File S6). This observation suggests that, in opaque cells, Stp1 plays a role in acute nitrogen starvation (in the absence of extracellular peptides or amino acids), while in white cells it does not appear to function in this way (Martínez and Ljungdahl 2005).

A strong prediction of Stp1 having a major role in the "induced" response of opaque cells is that the constitutively active Stp1 Δ2-61 allele (henceforth Stp1Δ2-61) (Martínez and Ljungdahl 2005) should phenocopy the opaque cell "induced" program in the absence of nitrogen starvation or proteins. We found that both white and opaque strains expressing Stp1Δ2-61 began logarithmic growth on BSA earlier (Figure S8C). In addition, both white and opaque cells expressing Stp1Δ2-61 in ammonium sulfate, our "basal" media condition, exhibit gene expression patterns similar to those of wild type cells proliferating on BSA as the sole nitrogen source, thereby confirming the prediction (Figure 6A lanes 6, 12–13, Figure 6B lanes 6–8, File S6).

Combining these results with transcriptional profiling of the *stp1* deletion and Stp1Δ2-61 strains, we can make the following conclusions regarding the role of Stp1 in the opaque cell induced response (Figure 6C). (1) Stp1 is the main regulator of the peptide transporters (*OPT2*, *OPT5*, *PTR2*) during the response of opaque cells to proteins as the sole nitrogen source (Figure 6A lanes 6–10, 12–13, File S6). (2) Stp1, Efg1, Wor3, and Csr1 are all needed for the full activation of *SAP1*, *SAP2*, *SAP3*, and *SAP8* in response to protein as the sole nitrogen source (Figure 6A lanes 6, 10, 12–13, Figure S9 lanes 3 and 5, and File S6).

To further understand the interplay between Stp1 and the other three regulators (Csr1, Efg1, Wor3), we transcriptionally profiled opaque *csr1*, *efg1*, and *wor3* strains expressing the Stp1Δ2-61 allele on either ammonium sulfate or BSA as the sole nitrogen source (Figure 6A lanes 12–19, File S6). On ammonium sulfate, we found that a portion of the expression pattern produced by the Stp1Δ2-61 allele (induction of *SAP1*, *SAP2*, and *SAP3*) depends on *EFG1* and *WOR3* but not *CSR1* (Figure 6A lanes 12, 14–16, File S6). In BSA as the sole nitrogen source, upregulation of *SAP1* (and *SAP3* to a lesser extent) depends on *EFG1* and *WOR3* while the induction of all four of the major *SAP*s depended, at least to some extent, on *CSR1* (Figure 6A lanes 13, 17–19, File S6). In contrast to opaque cells, deletion of *CSR1*, *EFG1*, or *WOR3* in white cells expressing the Stp1Δ2-61 allele had minimal, if any, effects on the white cell expression pattern (Figure 6B lanes 7–13, File S6).

To summarize, (1) Stp1 is needed to induce both the SAP and transporter genes when opaque cells use proteins as a sole nitrogen source (Figure 6A, Figure S9, and File S6). (2) Wor3 and Efg1 are needed for both the basal and induced responses in opaque cells while Csr1 is needed only for the induced response (Figure 6A and File S6). We conclude from

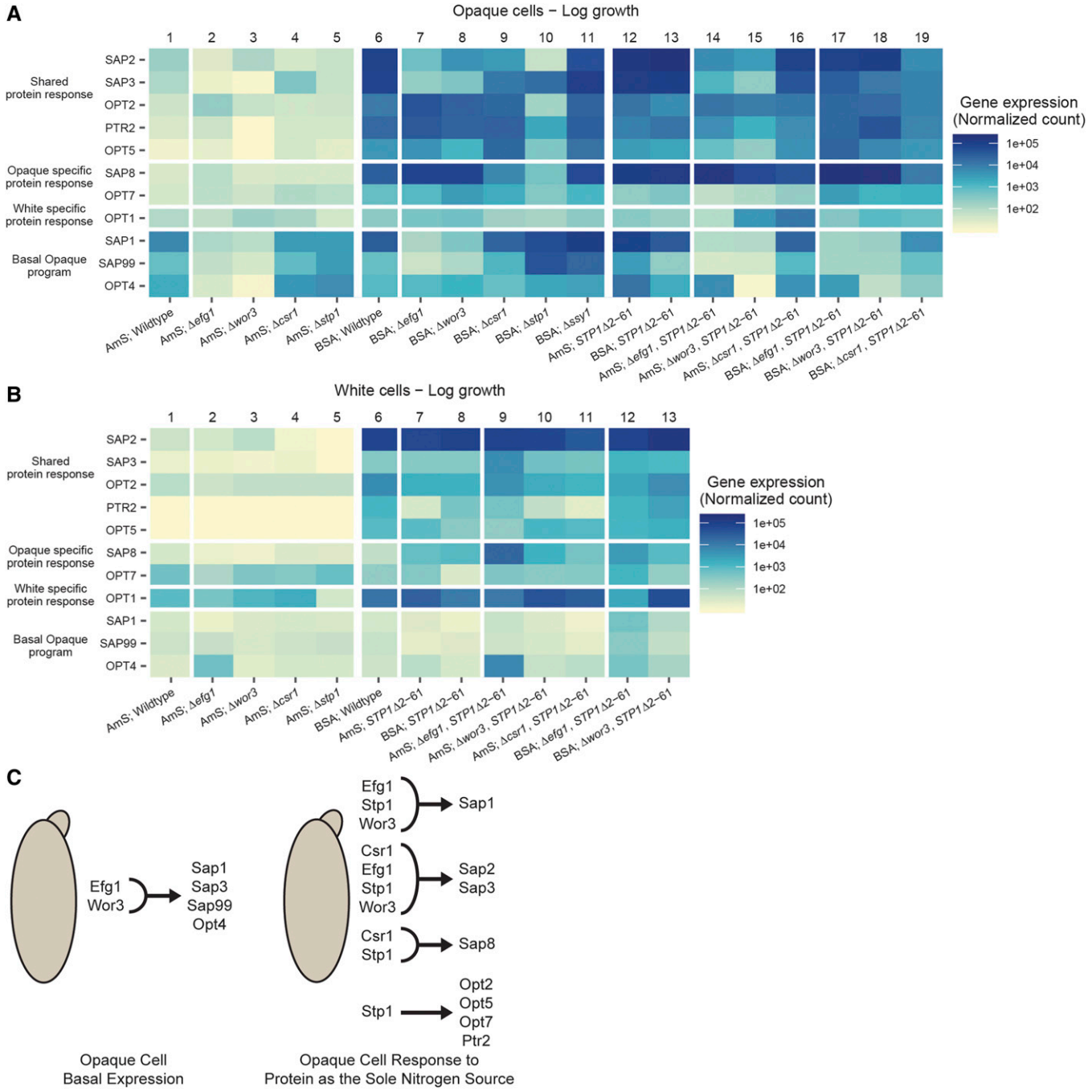

Figure 6 In opaque cells, four transcriptional regulators are necessary for either basal proteolytic activity, gene induction in response to proteins as a nitrogen source, or proliferation when proteins are the sole nitrogen source. (A and B) Transcript levels of selected genes in (A) opaque or (B) white cells of indicated genetic backgrounds growing on media where ammonium sulfate or protein (BSA) are the sole nitrogen sources. Average transcript levels for all replicates of each condition are plotted. Efg1 and Wor3, but not Csr1 or Stp1, are necessary for the basal opaque cell *SAP* and transporter expression profile when ammonium sulfate is the sole nitrogen source. Stp1, Wor3, Efg1, and Csr1 are needed for the full elaboration of the *SAP* component of the response to proteins in opaque cells. (C) Summary of the roles of Stp1, Efg1, Wor3, and Csr1 in the regulation of the basal opaque and opaque protein as sole nitrogen-source-induced expression of *SAP*s and transporters.

these experiments that activation of Stp1 is the key initiating event in both the white and opaque cell responses to protein as the sole nitrogen source, but that Wor3, Efg1, and Csr1 are needed for the full elaboration of the response in opaque cells (Figure 6C).

In opaque cells, Stp1 activation does not depend on Ssy1

Stp1 activation in white cells is dependent on the membrane bound sensor Ssy1 (Csy1), which is one of three components of the Ssy1p-Ptr3p-Ssy5p (SPS) sensor (Forsberg and

Ljungdahl 2001). Deletion of *SSY1* in white cells blocks Stp1 truncation, and thus activation, in response to extracellular amino acids (Martínez and Ljungdahl 2005). We deleted *SSY1* to determine if it was also necessary for the opaque cell induced response. Although proliferation of an opaque *ssy1* deletion strain on BSA as the sole nitrogen source was slightly delayed (roughly 24–36 hr *vs.* 18–24 hr) and slower (doubling every 4.5 *vs.* 4 hr) than wild type (Figure S8B and File S5), we found that the transcriptional profile of opaque *ssy1* deletion cells growing logarithmically on BSA was similar to that of wild type opaque cells (and the Stp1Δ2-61 strain) rather than the *stp1* deletion strain (Figure 6A lanes 6, 10–13 and File S6). Thus, we conclude that the full transcriptional response of opaque cells to protein as the sole nitrogen source requires Stp1, Wor3, Efg1, and Csr1 but not Ssy1, while the more limited response in white cells requires Stp1 and Ssy1 but not the other three regulators. It remains to be determined, however, whether the Ssy1-independent mechanism utilizes the other components of the SPS sensor (Ptr3/Ssy5) or an entirely different signaling pathway.

A minority opaque cell population supports white cell proliferation on BSA as a sole nitrogen source

We tested whether the induction of the *SAP*s in opaque cells could help white cells utilize BSA as a sole nitrogen source by co-incubating white and opaque cells tagged with different fluorescent markers and tracking the proliferation of each cell type over several days using flow cytometry (Figure 7A). In the presence of BSA as the sole nitrogen source, pure opaque cell and white cell populations began logarithmic proliferation after ~24 and 60–72 hr, respectively, with the proliferation rate, once the cells begin to divide, being faster in opaque cells (doubling every 3.5–4.5 hr *vs.* every 6–9 hr) (Figure 7B and File S5). These results are consistent with those described earlier based on single strain measurements (Figure 2A), indicating that the fluorescent markers did not significantly affect the relative growth rates. In populations that contained 20% opaque cells and 80% white cells, both cell types began proliferation after 24–36 hr and both proliferated at more similar rates (Figure 7B and File S5). Even a small fraction of opaque cells (<5%) had a significant effect on white cell proliferation in the presence of BSA as the sole nitrogen source, and we found that the maximum proliferation rate of white cells increased with the fraction of opaque cells (Figure 7B and File S5). The early proliferation of white cells did not occur when they were cocultured with the opaque quintuple *SAP* deletion strain, indicating that the increase in white cell proliferation in cocultures was dependent on Saps secreted by opaque cells (Figure S10 and File S5).

To further explore this "helping" effect, we asked whether wild type opaque cells could rescue the opaque quintuple *SAP* deletion strain or the opaque *stp1* deletion strain, neither of which can efficiently utilize BSA as the sole nitrogen source. We found that wild type opaque cells could completely rescue the quintuple *SAP* deletion strain (which actually proliferated slightly faster than wild type, doubling every 2.9 *vs.* 3.2 hr), and could partially rescue the *stp1* deletion strain (which doubled every 5.8 hr) (Figure S10 and File S5). These observations suggest that the growth defect of the quintuple *SAP* deletion stems solely from a lack of SAP-cleaved peptides rather than a more general inability to efficiently utilize peptides. Given that the opaque *stp1* deletion strain fails to induce the peptide transporters (*OPT2*, *OPT5*, *PTR2*), we interpret its inability to be fully rescued as a failure to take up BSA cleavage products. The increased proliferation rates of the quintuple *SAP* deletion strain and several of the quadruple *SAP* deletion strains relative to the parental strain on BSA suggests that there may be a fitness cost associated with the burden of expressing and secreting *SAP*s at high levels (File S5).

Our coculture experiments suggest that the receiving cells must actively respond in order to take full advantage of Sap cleavage products. To test this idea, we determined whether white cells mounted a specific response to BSA as a sole nitrogen source only in the presence of opaque cells. We performed coculture experiments with a GFP tagged wild type opaque strain and white strains with mCherry reporters driven by the *OPT1*, *OPT2*, *SAP2*, or *UGA4* promoters. In pure populations of white cells exposed to BSA as the sole nitrogen source, neither *SAP2* nor *OPT1* expression is fully upregulated within 60 hr and, conversely, *OPT2* and *UGA4* (which are induced simply by nitrogen starvation) are upregulated within 18 hr and remain fully induced after 60 hr (Figure 7C and Figure S11A). In the presence of wild type opaque cells, however, there is a noticeable increase in *SAP2* expression after 19 hr, which continues to increase until it is fully expressed in all white cells by 42 hr (Figure 7C). Likewise, *OPT1* levels begin to increase (relative to a pure white cell population) within 18 hr and appear fully induced within 24 hr (Figure S11A). Expression of *OPT2* and *UGA4*, on the other hand, noticeably begins to decrease (relative to a pure white cell population) after 18–24 hr and reached their local minimum within 42 hr in the presence of opaque cells (Figure 7C and Figure S11A). These results indicate that not only does the presence of opaque cells allow white cells to proliferate in the presence of BSA as the sole nitrogen source, but that the white cells respond differently (and sooner) to BSA as the sole nitrogen source in the presence of opaque cells.

The results of these experiments do not distinguish whether the "signal" from opaque to white cells is simply the presence of BSA cleavage products or some other molecule secreted by opaque cells. To answer this question, white cells were incubated with BSA that had been pretreated with proteinase K, and we observed upregulation of *SAP2* and *OPT1* and downregulation of *UGA4* relative to levels in white cells exposed to intact BSA (Figure S11B). This result argues strongly that, in the coculture experiments, BSA peptides produced by opaque cells are the signal for white cells to respond.

To test whether the helping effect of opaque cells for white cells extended across species, we performed similar coculture experiments with *C. dubliniensis*, *C. tropicalis*, and *C. parapsilosis*, none of which can efficiently utilize BSA as the sole nitrogen source (Figure S12). All three of these species

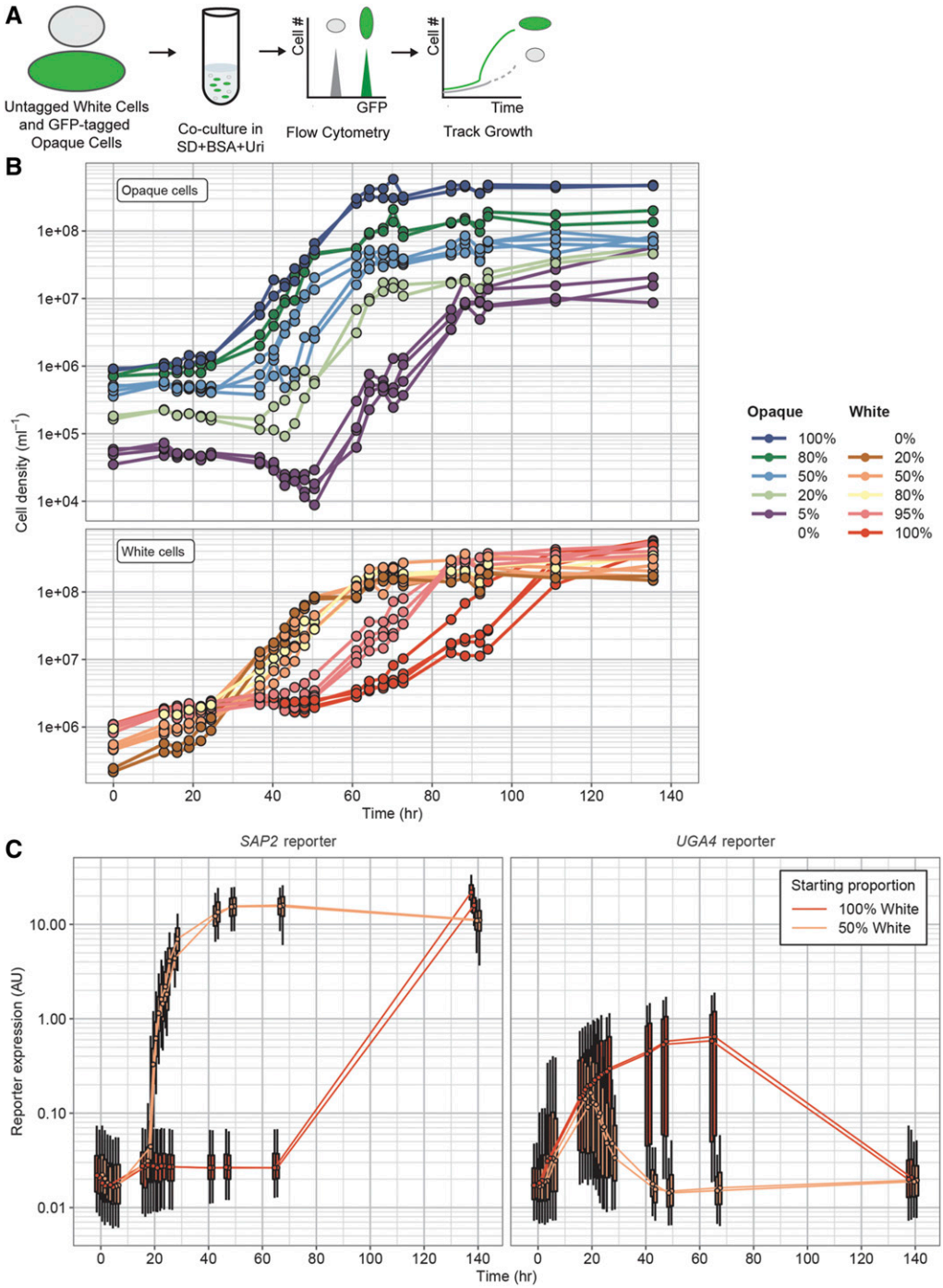

Figure 7 White cells more rapidly utilize BSA as a sole nitrogen source in the presence of opaque cells. (A) Different ratios of GFP-tagged opaque cells and untagged white cells were cocultured in SD+BSA+Uri media at 25°. Changes in cell density were measured by flow cytometry over the course of several days and the two cell types were distinguished by GFP fluorescence. (B) Proliferation of opaque (top) and white (bottom) cells grown by themselves or cocultured at different ratios when BSA is the sole nitrogen source. Cell counts and GFP fluorescence were determined by flow cytometry. Experimental data shown for experiments with white cell Tef2-mCherry/opaque cell Tef2-GFP and with white cell Tef2-GFP/opaque cell Tef2-mCherry pairings, in both cases the two cell types were distinguished based on GFP expression. Each line represents an individual experiment. (C) Expression of a mCherry reporter driven by the *SAP2* (left) or *UGA4* (right) promoter in white cells, grown by themselves (red) or with an equal number of Tef2-GFP expressing opaque cells (orange), when BSA is the sole nitrogen source. Boxes indicate the 25th to 75th percentiles of the data and whiskers indicate the 5th to 95th percentiles of the data for each sample at each time point. mCherry fluorescence was determined by flow cytometry and normalized by side scatter. White and opaque cells were distinguished based on the GFP expressed by opaque cells.

showed significantly improved proliferation when cocultured with wild type opaque *C. albicans* (Figure S12), but not with wild type white *C. albicans* cells (Figure S12).

Discussion

C. albicans—a fungal component of the human microbiome and an opportunistic pathogen of humans—can switch between two heritable states, called white and opaque. In this paper, we identify a highly inducible gene expression program specific to opaque cells (both in terms of specific genes and in the magnitude of the response), which enables them to efficiently utilize proteins as a sole source of nitrogen. We demonstrate, using proteomics, multiplex protease substrate profiling, and transcriptional analysis, that a series of secreted aspartyl proteases (SAPs) are constitutively secreted by opaque cells, comprising almost half of the secreted proteins. When protein is present as the sole nitrogen source, some of these *SAP*s (which are already expressed at high levels) are induced even further, along with a group of other

genes including specific peptide transporters. We show that the protein-induced response is not simply an upregulation of the basal pattern, as other genes are also activated to produce an entirely new pattern of gene expression. We show that these secreted proteases degrade generic proteins, whose peptides can then be used as a nitrogen source. As a result, opaque cells proliferate faster than white cells in media where protein is the sole nitrogen source; in nearly all other types of media, white cells outcompete opaque cells. Using deletion mutants, we identified the individual *SAP*s required for opaque cells to efficiently utilize protein as a nitrogen source. In contrast to white cells, where a single *SAP* (*SAP2*) allows limited growth under these conditions (Hube *et al.* 1997), upregulation of any one of four opaque-induced *SAP*s (*SAP1*, *SAP2*, *SAP3*, *SAP8*) can suffice for efficient proliferation of opaque cells. Activation of Stp1—a previously identified regulator of *SAP* genes in white cells (Martínez and Ljungdahl 2005)—is also key for the opaque-specific upregulation, although the response differs greatly between white and opaque cells. Compared to white cells, opaque cells appear to activate Stp1 in a different way, and have incorporated at least three additional regulators (Wor3, Efg1, and Csr1) that act in concert with Stp1. It seems likely that these differences contribute to both the timing of the response in opaque cells as well as its magnitude.

White and opaque cells differ in many properties, and are often thought of as being specialized for different niches in their mammalian hosts. In this work, we show that, in mixed cultures of white and opaque cells, a minority of opaque cells, by providing massive amounts of secreted proteases, can benefit the entire culture. This result suggests that, rather than occupying separate niches in the host, the two types of cells can work together to produce a population that can be robust to changing environments. White and opaque cells carry identical genomes, and it is an intriguing idea that *C. albicans*' ability to adapt to a wide range of environments might be achieved, at least in part, by partitioning expression of the genome between two different types of cooperating cells, where each cell type has specific, but complementary, metabolic characteristics. In the case examined here, a small subpopulation of opaque cells could shoulder the burden of expressing *SAP*s at high levels, allowing white cells to thrive when proteins are the sole nitrogen source.

Such a partnership need not be limited to nitrogen acquisition, it could extend to a wide-range of other *SAP*-mediated functions (*e.g.*, interactions with bacteria (Dutton *et al.* 2016), adhesion to host cells (Watts *et al.* 1998; Bektic *et al.* 2001; Albrecht *et al.* 2006), protection from host defense proteins (Borg-von Zepelin *et al.* 1998; Gropp *et al.* 2009; Meiller *et al.* 2009; Rapala-Kozik *et al.* 2010, 2015; Bochenska *et al.* 2015; Kozik *et al.* 2015), and activation of immune responses (Schaller *et al.* 2005; Hornbach *et al.* 2009; Pietrella *et al.* 2010; Pericolini *et al.* 2015; Gabrielli *et al.* 2016)). Additionally, white and opaque cells differ in many more ways than their patterns of *SAP* expression; for example, differences have been observed in cell wall associated proteins, metabolite production and use, and the responses to specific environmental cues, suggesting other possibilities for collaboration between the cell types. Our proteomics experiments showed preferential secretion of the phospholipase Plb4.5 by white cells and the acid phosphatase Pho112 by opaque cells, suggesting a specific testable example.

Finally, we note that the benefits of *SAP*-mediated nitrogen acquisition by opaque cells are not limited to *C. albicans*. We showed that three other species (*C. dubliniensis*, *C. tropicalis*, and *C. parapsilosis*), each of which, on its own, cannot efficiently proliferate on BSA as a sole nitrogen source, can do so in the presence of *C. albicans* opaque cells. There is no *a priori* reason that more distantly related fungi, or even bacteria, with the capacity to uptake and process short peptides could not also benefit from the presence of *C. albicans* opaque cells.

Acknowledgments

We thank Haley Gause, Carrie Graham, and Niyati Rodricks for advice. We thank Ananda Mendoza for technical support. Support was provided by the University of California San Francisco (UCSF) Mass Spectrometry Facility (A.L. Burlingame, Director) supported by the Dr. Miriam And Sheldon G. Adelson Medical Research Foundation (AMRF) and the National Institutes of Health (NIH) – National Institute of General Medical Sciences (NIGMS) NIH P41GM103481. This work was supported by NIH grants F32CA168150 (to M.B.W.), P50AI150476 (to C.S.C.) and R01AI049187 (to A.D.J.). This investigation has also been aided by a grant from The Jane Coffin Childs Memorial Fund for Medical Research (to N.Z.). The content is the sole responsibility of the authors and does not represent the views of the NIH or other funding agencies. Neither the NIH nor other funding agencies had any role in the design of the study, in the collection, analyses, or interpretation of data, in the writing of the manuscript, or in the decision to publish the results. Alexander D. Johnson is a cofounder of BioSynesis, Inc., a company developing inhibitors and diagnostics of *C. albicans* biofilms. Matthew Lohse was formerly an employee and currently is a consultant for BioSynesis, Inc.

Literature Cited

Achkar, J. M., and B. C. Fries, 2010 *Candida* infections of the genitourinary tract. Clin. Microbiol. Rev. 23: 253–273. https://doi.org/10.1128/CMR.00076-09

Albrecht, A., A. Felk, I. Pichová, J. R. Naglik, M. Schaller *et al.*, 2006 Glycosylphosphatidylinositol-anchored proteases of *Candida albicans* target proteins necessary for both cellular processes and host-pathogen interactions. J. Biol. Chem. 281: 688–694. https://doi.org/10.1074/jbc.M509297200

Anderson, M. Z., A. M. Porman, N. Wang, E. Mancera, D. Huang *et al.*, 2016 A multistate toggle switch defines fungal cell fates and is regulated by synergistic genetic cues. PLoS Genet. 12: e1006353. https://doi.org/10.1371/journal.pgen.1006353

Aoki, W., N. Kitahara, N. Miura, H. Morisaka, Y. Yamamoto *et al.*, 2011 Comprehensive characterization of secreted aspartic

proteases encoded by a virulence gene family in *Candida albicans*. J. Biochem. 150: 431–438. https://doi.org/10.1093/jb/mvr073

Bektic, J., C. P. Lell, A. Fuchs, H. Stoiber, C. Speth *et al*., 2001 HIV protease inhibitors attenuate adherence of *Candida albicans* to epithelial cells *in vitro*. FEMS Immunol. Med. Microbiol. 31: 65–71. https://doi.org/10.1111/j.1574-695X.2001.tb01588.x

Bergen, M. S., E. Voss, and D. R. Soll, 1990 Switching at the cellular level in the white-opaque transition of *Candida albicans*. J. Gen. Microbiol. 136: 1925–1936. https://doi.org/10.1099/00221287-136-10-1925

Blom, A. M., T. Hallström, and K. Riesbeck, 2009 Complement evasion strategies of pathogens-acquisition of inhibitors and beyond. Mol. Immunol. 46: 2808–2817. https://doi.org/10.1016/j.molimm.2009.04.025

Bochenska, O., M. Rapala-Kozik, N. Wolak, W. Kamysz, D. Grzywacz *et al*., 2015 Inactivation of human kininogen-derived antimicrobial peptides by secreted aspartic proteases produced by the pathogenic yeast *Candida albicans*. Biol. Chem. 396: 1369–1375. https://doi.org/10.1515/hsz-2015-0167

Borg-von Zepelin, M., S. Beggah, K. Boggian, D. Sanglard, and M. Monod, 1998 The expression of the secreted aspartyl proteinases Sap4 to Sap6 from *Candida albicans* in murine macrophages. Mol. Microbiol. 28: 543–554. https://doi.org/10.1046/j.1365-2958.1998.00815.x

Calderone, R. A., and W. A. Fonzi, 2001 Virulence factors of *Candida albicans*. Trends Microbiol. 9: 327–335. https://doi.org/10.1016/S0966-842X(01)02094-7

Chalkley, R. J., P. R. Baker, K. F. Medzihradszky, A. J. Lynn, and A. L. Burlingame, 2008 In-depth analysis of tandem mass spectrometry data from disparate instrument types. Mol. Cell. Proteomics 7: 2386–2398. https://doi.org/10.1074/mcp.M800021-MCP200

Colaert, N., K. Helsens, L. Martens, J. Vandekerckhove, and K. Gevaert, 2009 Improved visualization of protein consensus sequences by iceLogo. Nat. Methods 6: 786–787. https://doi.org/10.1038/nmeth1109-786

Dalal, C. K., I. A. Zuleta, M. B. Lohse, R. E. Zordan, H. El-Samad *et al*., 2019 A population shift between two heritable cell types of the pathogen *Candida albicans* is based both on switching and selective proliferation. Proc. Natl. Acad. Sci. USA 116: 26918–26924. https://doi.org/10.1073/pnas.1908986116

Diggle, S. P., A. S. Griffin, G. S. Campbell, and S. A. West, 2007 Cooperation and conflict in quorum-sensing bacterial populations. Nature 450: 411–414. https://doi.org/10.1038/nature06279

Dunkel, N., T. Hertlein, R. Franz, O. Reuss, C. Sasse *et al*., 2013 Roles of different peptide transporters in nutrient acquisition in *Candida albicans*. Eukaryot. Cell 12: 520–528. https://doi.org/10.1128/EC.00008-13

Dutton, L. C., H. F. Jenkinson, R. J. Lamont, and A. H. Nobbs, 2016 Role of *Candida albicans* secreted aspartyl protease Sap9 in interkingdom biofilm formation. Pathog. Dis. 74: ftw005. https://doi.org/10.1093/femspd/ftw005

Eggimann, P., J. Garbino, and D. Pittet, 2003 Epidemiology of *Candida* species infections in critically ill non-immunosuppressed patients. Lancet Infect. Dis. 3: 685–702. https://doi.org/10.1016/S1473-3099(03)00801-6

Ellis B., P. Haaland, F. Hahne, N. Le Meur, N. Gopalakrishnan, *et al.*, 2019 flowCore: Basic structures for flow cytometry data. R package version 1.50.0.

Ene, I. V., M. B. Lohse, A. V. Vladu, J. Morschhäuser, A. D. Johnson *et al*., 2016 Phenotypic profiling reveals that *Candida albicans* opaque cells represent a metabolically specialized cell state compared to default white cells. MBio 7: e01269-e16. https://doi.org/10.1128/mBio.01269-16

Felk, A., M. Kretschmar, A. Albrecht, M. Schaller, S. Beinhauer *et al*., 2002 *Candida albicans* hyphal formation and the expression of the Efg1-regulated proteinases Sap4 to Sap6 are required for the invasion of parenchymal organs. Infect. Immun. 70: 3689–3700. https://doi.org/10.1128/IAI.70.7.3689-3700.2002

Forsberg, H., and P. O. Ljungdahl, 2001 Genetic and biochemical analysis of the yeast plasma membrane Ssy1p-Ptr3p-Ssy5p sensor of extracellular amino acids. Mol. Cell. Biol. 21: 814–826. https://doi.org/10.1128/MCB.21.3.814-826.2001

Gabrielli, E., S. Sabbatini, E. Roselletti, L. Kasper, S. Perito *et al*., 2016 *In vivo* induction of neutrophil chemotaxis by secretory aspartyl proteinases of *Candida albicans*. Virulence 7: 819–825. https://doi.org/10.1080/21505594.2016.1184385

Geiger, J., D. Wessels, S. R. Lockhart, and D. R. Soll, 2004 Release of a potent polymorphonuclear leukocyte chemoattractant is regulated by white-opaque switching in *Candida albicans*. Infect. Immun. 72: 667–677. https://doi.org/10.1128/IAI.72.2.667-677.2004

Gropp, K., L. Schild, S. Schindler, B. Hube, P. F. Zipfel *et al*., 2009 The yeast *Candida albicans* evades human complement attack by secretion of aspartic proteases. Mol. Immunol. 47: 465–475. https://doi.org/10.1016/j.molimm.2009.08.019

Gudlaugsson, O., S. Gillespie, K. Lee, J. Vande Berg, J. Hu *et al*., 2003 Attributable mortality of nosocomial candidemia, revisited. Clin. Infect. Dis. 37: 1172–1177. https://doi.org/10.1086/378745

Guerin, M., N. Camougrand, R. Caubet, S. Zniber, G. Velours *et al*., 1989 The second respiratory chain of *Candida parapsilosis*: a comprehensive study. Biochimie 71: 887–902. https://doi.org/10.1016/0300-9084(89)90072-2

Hernday, A. D., M. B. Lohse, P. M. Fordyce, C. J. Nobile, J. D. DeRisi *et al*., 2013 Structure of the transcriptional network controlling white-opaque switching in *Candida albicans*. Mol. Microbiol. 90: 22–35.

Hornbach, A., A. Heyken, L. Schild, B. Hube, J. Löffler *et al*., 2009 The glycosylphosphatidylinositol-anchored protease Sap9 modulates the interaction of *Candida albicans* with human neutrophils. Infect. Immun. 77: 5216–5224. https://doi.org/10.1128/IAI.00723-09

Hube, B., M. Monod, D. A. Schofield, A. J. P. Brown, and N. A. R. Gow, 1994 Expression of seven members of the gene family encoding secretory aspartyl proteinases in *Candida albicans*. Mol. Microbiol. 14: 87–99. https://doi.org/10.1111/j.1365-2958.1994.tb01269.x

Hube, B., D. Sanglard, F. C. Odds, D. Hess, M. Monod *et al*., 1997 Disruption of each of the secreted aspartyl proteinase genes *SAP1*, *SAP2*, and *SAP3* of *Candida albicans* attenuates virulence. Infect. Immun. 65: 3529–3538. https://doi.org/10.1128/IAI.65.9.3529-3538.1997

Johnson, A., 2003 The biology of mating in *Candida albicans*. Nat. Rev. Microbiol. 1: 106–116. https://doi.org/10.1038/nrmicro752

Joly, S., C. Pujol, K. Schröppel, and D. R. Soll, 1996 Development of two species-specific fingerprinting probes for broad computer-assisted epidemiological studies of *Candida tropicalis*. J. Clin. Microbiol. 34: 3063–3071. https://doi.org/10.1128/JCM.34.12.3063-3071.1996

Kennedy, M. J., and P. A. Volz, 1985 Ecology of *Candida albicans* gut colonization: inhibition of *Candida* adhesion, colonization, and dissemination from the gastrointestinal tract by bacterial antagonism. Infect. Immun. 49: 654–663. https://doi.org/10.1128/IAI.49.3.654-663.1985

Kim, J., and P. Sudbery, 2011 *Candida albicans*, a major human fungal pathogen. J. Microbiol. 49: 171–177. https://doi.org/10.1007/s12275-011-1064-7

Koelsch, G., J. Tang, J. A. Loy, M. Monod, K. Jackson *et al*., 2000 Enzymic characteristics of secreted aspartic proteases of *Candida albicans*. Biochim. Biophys. Acta 1480: 117–131. https://doi.org/10.1016/S0167-4838(00)00068-6

Korting, H. C., B. Hube, S. Oberbauer, E. Januschke, G. Hamm *et al*., 2003 Reduced expression of the hyphal-independent *Candida*

albicans proteinase genes *SAP1* and *SAP3* in the *efg1* mutant is associated with attenuated virulence during infection of oral epithelium. J. Med. Microbiol. 52: 623–632. https://doi.org/10.1099/jmm.0.05125-0

Koziel, J., and J. Potempa, 2013 Protease-armed bacteria in the skin. Cell Tissue Res. 351: 325–337. https://doi.org/10.1007/s00441-012-1355-2

Kozik, A., M. Gogol, O. Bochenska, J. Karkowska-Kuleta, N. Wolak *et al.*, 2015 Kinin release from human kininogen by 10 aspartic proteases produced by pathogenic yeast *Candida albicans*. BMC Microbiol. 15: 60. https://doi.org/10.1186/s12866-015-0394-8

Kullberg, B. J., and A. M. L. Oude Lashof, 2002 Epidemiology of opportunistic invasive mycoses. Eur. J. Med. Res. 7: 183–191.

Kumamoto, C. A., 2011 Inflammation and gastrointestinal *Candida* colonization. Curr. Opin. Microbiol. 14: 386–391. https://doi.org/10.1016/j.mib.2011.07.015

Kvaal, C. A., T. Srikantha, and D. R. Soll, 1997 Misexpression of the white-phase-specific gene *WH11* in the opaque phase of *Candida albicans* affects switching and virulence. Infect. Immun. 65: 4468–4475. https://doi.org/10.1128/IAI.65.11.4468-4475.1997

Kvaal, C., S. A. Lachke, T. Srikantha, K. Daniels, J. McCoy *et al.*, 1999 Misexpression of the opaque-phase-specific gene *PEP1* (*SAP1*) in the white phase of *Candida albicans* confers increased virulence in a mouse model of cutaneous infection. Infect. Immun. 67: 6652–6662. https://doi.org/10.1128/IAI.67.12.6652-6662.1999

Lan, C., G. Newport, L. Murillo, T. Jones, S. Scherer *et al.*, 2002 Metabolic specialization associated with phenotypic switching in *Candida albicans*. Proc. Natl. Acad. Sci. USA 99: 14907–14912. https://doi.org/10.1073/pnas.232566499

Lin, C. H., S. Kabrawala, E. P. Fox, C. J. Nobile, A. D. Johnson *et al.*, 2013 Genetic control of conventional and pheromone-stimulated biofilm formation in *Candida albicans*. PLoS Pathog. 9: e1003305. https://doi.org/10.1371/journal.ppat.1003305

Lockhart, S. R., C. Pujol, K. J. Daniels, M. G. Miller, A. D. Johnson *et al.*, 2002 In *Candida albicans*, white-opaque switchers are homozygous for mating type. Genetics 162: 737–745.

Lohse, M. B., and A. D. Johnson, 2008 Differential phagocytosis of white versus opaque *Candida albicans* by *Drosophila* and mouse phagocytes. PLoS One 3: e1473. https://doi.org/10.1371/journal.pone.0001473

Lohse, M. B., and A. D. Johnson, 2009 White-opaque switching in *Candida albicans*. Curr. Opin. Microbiol. 12: 650–654. https://doi.org/10.1016/j.mib.2009.09.010

Lohse, M. B., and A. D. Johnson, 2016 Identification and characterization of Wor4, a new transcriptional regulator of white-opaque switching. G3 (Bethesda) 6: 721–729. https://doi.org/10.1534/g3.115.024885

Lohse, M. B., A. D. Hernday, P. M. Fordyce, L. Noiman, T. R. Sorrells *et al.*, 2013 Identification and characterization of a previously undescribed family of sequence-specific DNA-binding domains. Proc. Natl. Acad. Sci. USA 110: 7660–7665. https://doi.org/10.1073/pnas.1221734110

Lohse, M. B., I. V. Ene, V. B. Craik, A. D. Hernday, E. Mancera *et al.*, 2016 Systematic genetic screen for transcriptional regulators of the *Candida albicans* white-opaque switch. Genetics 203: 1679–1692. https://doi.org/10.1534/genetics.116.190645

Martínez, P., and P. O. Ljungdahl, 2005 Divergence of Stp1 and Stp2 transcription factors in *Candida albicans* places virulence factors required for proper nutrient acquisition under amino acid control. Mol. Cell. Biol. 25: 9435–9446. https://doi.org/10.1128/MCB.25.21.9435-9446.2005

Meiller, T. F., B. Hube, L. Schild, M. E. Shirtliff, M. A. Scheper *et al.*, 2009 A novel immune evasion strategy of *Candida albicans*: proteolytic cleavage of a salivary antimicrobial peptide. PLoS One 4: e5039. https://doi.org/10.1371/journal.pone.0005039

Miller, M. G., and A. D. Johnson, 2002 White-opaque switching in *Candida albicans* is controlled by mating-type locus homeodomain proteins and allows efficient mating. Cell 110: 293–302. https://doi.org/10.1016/S0092-8674(02)00837-1

Morschhäuser, J., 2010 Regulation of white-opaque switching in *Candida albicans*. Med. Microbiol. Immunol. (Berl.) 199: 165–172. https://doi.org/10.1007/s00430-010-0147-0

Nelson, G., and T. W. Young, 1986 Yeast extracellular proteolytic enzymes for chill-proofing beer. J. Inst. Brew. 92: 599–603. https://doi.org/10.1002/j.2050-0416.1986.tb04460.x

Nguyen, N., M. M. F. Quail, and A. D. Hernday, 2017 An efficient, rapid, and recyclable system for CRISPR-mediated genome editing in *Candida albicans*. MSphere 2: e00149-e17. https://doi.org/10.1128/mSphereDirect.00149-17

Noble, S. M., and A. D. Johnson, 2005 Strains and strategies for large-scale gene deletion studies of the diploid human fungal pathogen *Candida albicans*. Eukaryot. Cell 4: 298–309. https://doi.org/10.1128/EC.4.2.298-309.2005

O'Donoghue, A. J., A. A. Eroy-Reveles, G. M. Knudsen, J. Ingram, M. Zhou *et al.*, 2012 Global identification of peptidase specificity by multiplex substrate profiling. Nat. Methods 9: 1095–1100. https://doi.org/10.1038/nmeth.2182

O'Donoghue, A. J., G. M. Knudsen, C. Beekman, J. A. Perry, A. D. Johnson *et al.*, 2015 Destructin-1 is a collagen-degrading endopeptidase secreted by *Pseudogymnoascus destructans*, the causative agent of white-nose syndrome. Proc. Natl. Acad. Sci. USA 112: 7478–7483. https://doi.org/10.1073/pnas.1507082112

Pappas, P. G., J. H. Rex, J. D. Sobel, S. G. Filler, W. E. Dismukes *et al.*, 2004 Guidelines for treatment of candidiasis. Clin. Infect. Dis. 38: 161–189. https://doi.org/10.1086/380796

Park, Y., and J. Morschhäuser, 2005 Tetracycline-inducible gene expression and gene deletion in *Candida albicans*. Eukaryot. Cell 4: 1328–1342. https://doi.org/10.1128/EC.4.8.1328-1342.2005

Parra-Ortega, B., H. Cruz-Torres, L. Villa-Tanaca, and C. Hernández-Rodríguez, 2009 Phylogeny and evolution of the aspartyl protease family from clinically relevant *Candida* species. Mem. Inst. Oswaldo Cruz 104: 505–512. https://doi.org/10.1590/S0074-02762009000300018

Pericolini, E., E. Gabrielli, M. Amacker, L. Kasper, E. Roselletti *et al.*, 2015 Secretory aspartyl proteinases cause vaginitis and can mediate vaginitis caused by *Candida albicans* in mice. MBio 6: e00724. https://doi.org/10.1128/mBio.00724-15

Pietrella, D., A. Rachini, N. Pandey, L. Schild, M. Netea *et al.*, 2010 The inflammatory response induced by aspartic proteases of *Candida albicans* is independent of proteolytic activity. Infect. Immun. 78: 4754–4762. https://doi.org/10.1128/IAI.00789-10

Pietrocola, G., G. Nobile, S. Rindi, and P. Speziale, 2017 - *Staphylococcus aureus* manipulates innate immunity through own and host-expressed proteases. Front. Cell. Infect. Microbiol. 7: 166. https://doi.org/10.3389/fcimb.2017.00166

Porman, A. M., K. Alby, M. P. Hirakawa, and R. J. Bennett, 2011 Discovery of a phenotypic switch regulating sexual mating in the opportunistic fungal pathogen *Candida tropicalis*. Proc. Natl. Acad. Sci. USA 108: 21158–21163. https://doi.org/10.1073/pnas.1112076109

Priest, S. J., and M. C. Lorenz, 2015 Characterization of virulence-related phenotypes in *Candida species* of the CUG clade. Eukaryot. Cell 14: 931–940. https://doi.org/10.1128/EC.00062-15

Pujol, C., K. J. Daniels, S. R. Lockhart, T. Srikantha, J. B. Radke *et al.*, 2004 The closely related species *Candida albicans* and *Candida dubliniensis* can mate. Eukaryot. Cell 3: 1015–1027. https://doi.org/10.1128/EC.3.4.1015-1027.2004

R Core Team, 2019 *R: A language and environment for statistical computing*. R Foundation for Statistical Computing, Vienna, Austria, https://www.R-project.org/.

Rapala-Kozik, M., J. Karkowska-Kuleta, A. Ryzanowska, A. Golda, A. Barbasz *et al.*, 2010 Degradation of human kininogens with the release of kinin peptides by extracellular proteinases of *Candida* spp. Biol. Chem. 391: 823–830. https://doi.org/10.1515/bc.2010.083

Rapala-Kozik, M., O. Bochenska, M. Zawrotniak, N. Wolak, G. Trebacz *et al.*, 2015 Inactivation of the antifungal and immunomodulatory properties of human cathelicidin LL-37 by aspartic proteases produced by the pathogenic yeast *Candida albicans*. Infect. Immun. 83: 2518–2530. https://doi.org/10.1128/IAI.00023-15

Reuss, O., and J. Morschhäuser, 2006 A family of oligopeptide transporters is required for growth of *Candida albicans* on proteins. Mol. Microbiol. 60: 795–812. https://doi.org/10.1111/j.1365-2958.2006.05136.x

Rikkerink, E. H., B. B. Magee, and P. T. Magee, 1988 Opaque-white phenotype transition: a programmed morphological transition in *Candida albicans*. J. Bacteriol. 170: 895–899. https://doi.org/10.1128/JB.170.2.895-899.1988

Sasse, C., M. Hasenberg, M. Weyler, M. Gunzer, and J. Morschhäuser, 2013 White-opaque switching of *Candida albicans* allows immune evasion in an environment-dependent fashion. Eukaryot. Cell 12: 50–58. https://doi.org/10.1128/EC.00266-12

Schaller, M., H. C. Korting, C. Borelli, G. Hamm, and B. Hube, 2005 *Candida albicans*-secreted aspartic proteinases modify the epithelial cytokine response in an *in vitro* model of vaginal candidiasis. Infect. Immun. 73: 2758–2765. https://doi.org/10.1128/IAI.73.5.2758-2765.2005

Si, H., A. D. Hernday, M. P. Hirakawa, A. D. Johnson, and R. J. Bennett, 2013 *Candida albicans* white and opaque cells undergo distinct programs of filamentous growth. PLoS Pathog. 9: e1003210. https://doi.org/10.1371/journal.ppat.1003210

Slutsky, B., M. Staebell, J. Anderson, L. Risen, M. Pfaller *et al.*, 1987 "White-opaque transition": a second high-frequency switching system in *Candida albicans*. J. Bacteriol. 169: 189–197. https://doi.org/10.1128/JB.169.1.189-197.1987

Soll, D. R., 2009 Why does *Candida albicans* switch? FEMS Yeast Res. 9: 973–989. https://doi.org/10.1111/j.1567-1364.2009.00562.x

Soll, D. R., B. Morrow, and T. Srikantha, 1993 High-frequency phenotypic switching in *Candida albicans*. Trends Genet. 9: 61–65. https://doi.org/10.1016/0168-9525(93)90189-O

Sonneborn, A., B. Tebarth, and J. Ernst, 1999 Control of white-opaque phenotypic switching in *Candida albicans* by the Efg1p morphogenetic regulator. Infect. Immun. 67: 4655–4660. https://doi.org/10.1128/IAI.67.9.4655-4660.1999

Srikantha, T., B. Morrow, K. Schröppel, and D. R. Soll, 1995 The frequency of integrative transformation at phase-specific genes of *Candida albicans* correlates with their transcriptional state. Mol. Gen. Genet. 246: 342–352. https://doi.org/10.1007/BF00288607

Staib, F., 1965 Serum-proteins as nitrogen source for yeastlike fungi. Sabouraudia 4: 187–193. https://doi.org/10.1080/00362176685190421

Sullivan, D. J., T. J. Westerneng, K. A. Haynes, D. E. Bennett, and D. C. Coleman, 1995 *Candida dubliniensis* sp. nov.: phenotypic and molecular characterization of a novel species associated with oral candidosis in HIV-infected individuals. Microbiology 141: 1507–1521. https://doi.org/10.1099/13500872-141-7-1507

Takagi, J., S. D. Singh-Babak, M. B. Lohse, C. K. Dalal, and A. D. Johnson, 2019 *Candida albicans* white and opaque cells exhibit distinct spectra of organ colonization in mouse models of infection. PLoS One 14: e0218037. https://doi.org/10.1371/journal.pone.0218037

Tuch, B. B., Q. M. Mitrovich, O. R. Homann, A. D. Hernday, C. K. Monighetti *et al.*, 2010 The transcriptomes of two heritable cell types illuminate the circuit governing their differentiation. PLoS Genet. 6: e1001070. https://doi.org/10.1371/journal.pgen.1001070

Van, P., W. Jiang, R. Gottardo, and G. Finak, 2018 ggCyto: next generation open-source visualization software for cytometry. Bioinformatics 34: 3951–3953. https://doi.org/10.1093/bioinformatics/bty441

Vylkova, S., A. J. Carman, H. A. Danhof, J. R. Collette, H. Zhou *et al.*, 2011 The fungal pathogen *Candida albicans* autoinduces hyphal morphogenesis by raising extracellular pH. MBio 2: e00055-11. https://doi.org/10.1128/mBio.00055-11

Watts, H. J., F. S. Cheah, B. Hube, D. Sanglard, and N. A. Gow, 1998 Altered adherence in strains of *Candida albicans* harbouring null mutations in secreted aspartic proteinase genes. FEMS Microbiol. Lett. 159: 129–135. https://doi.org/10.1111/j.1574-6968.1998.tb12851.x

Wenzel, R. P., 1995 Nosocomial candidemia: risk factors and attributable mortality. Clin. Infect. Dis. 20: 1531–1534. https://doi.org/10.1093/clinids/20.6.1531

Wey, S. B., M. Mori, M. A. Pfaller, R. F. Woolson, and R. P. Wenzel, 1988 Hospital-acquired candidemia. The attributable mortality and excess length of stay. Arch. Intern. Med. 148: 2642–2645. https://doi.org/10.1001/archinte.1988.00380120094019

White, T. C., and N. Agabian, 1995 *Candida albicans* secreted aspartyl proteinases: isoenzyme pattern is determined by cell type, and levels are determined by environmental factors. J. Bacteriol. 177: 5215–5221. https://doi.org/10.1128/JB.177.18.5215-5221.1995

White, R. C., F. F. Gunderson, J. Y. Tyson, K. H. Richardson, T. J. Portlock *et al.*, 2018 Type II secretion-dependent aminopeptidase LapA and acyltransferase PlaC are redundant for nutrient acquisition during *Legionella pneumophila* intracellular infection of amoebas. MBio 9: e00528-18. https://doi.org/10.1128/mBio.00528-18

Wickham, H., 2017 tidyverse: Easily Install and Load the "Tidyverse." R Package Version 1.2.1 https://CRAN.R-project.org/package=tidyverse.

Winter, M. B., E. C. Salcedo, M. B. Lohse, N. Hartooni, M. Gulati *et al.*, 2016 Global identification of biofilm-specific proteolysis in *Candida albicans*. MBio 7: e01514-16. https://doi.org/10.1128/mBio.01514-16

Winter, M. B., F. La Greca, S. Arastu-Kapur, F. Caiazza, P. Cimermancic *et al.*, 2017 Immunoproteasome functions explained by divergence in cleavage specificity and regulation. eLife 6: e27364. https://doi.org/10.7554/eLife.27364

Ziv, N., M. L. Siegal, and D. Gresham, 2013 Genetic and nongenetic determinants of cell growth variation assessed by high-throughput microscopy. Mol. Biol. Evol. 30: 2568–2578. https://doi.org/10.1093/molbev/mst138

Zordan, R. E., D. J. Galgoczy, and A. D. Johnson, 2006 Epigenetic properties of white-opaque switching in *Candida albicans* are based on a self-sustaining transcriptional feedback loop. Proc. Natl. Acad. Sci. USA 103: 12807–12812. https://doi.org/10.1073/pnas.0605138103

Zordan, R., M. Miller, D. Galgoczy, B. Tuch, and A. Johnson, 2007 Interlocking transcriptional feedback loops control white-opaque switching in *Candida albicans*. PLoS Biol. 5: e256. https://doi.org/10.1371/journal.pbio.0050256

Communicating editor: A. Hinnebusch